

TUTORIAL

Squeezed states of light

M C Teich† and B E A Saleh‡

†Columbia University, New York, New York 10027, USA

‡University of Wisconsin, Madison, Wisconsin 53706, USA

Received 17 August 1989, in final form 18 September 1989

Abstract. In this tutorial article we provide a discussion of squeezed states of light from an elementary point of view. An outline of the topics considered is provided in the contents list below. Following the presentation of topics 1–3, which are of a general nature, we discuss two kinds of nonclassical light: quadrature-squeezed light (topics 4–6) and photon-number-squeezed light (topics 7–9). In the last part of the article we provide a listing of early nonclassical light experiments and consider a number of applications (and potential applications) of squeezed light. Finally, we provide a survey of the available general literature.

Contents

1. Review of uncertainties in light
2. Examples of states of light
3. Definitions of squeezed-state light
4. Examples of quadrature-squeezed light
5. Detection of quadrature-squeezed light
6. Generation of quadrature-squeezed light
7. Examples of photon-number-squeezed light
8. Detection of photon-number-squeezed light
9. Generation of photon-number-squeezed light
10. Early nonclassical light experiments
11. Applications of squeezed light
12. Available general literature

1. Review of uncertainties in light

Consider monochromatic light from a classical point of view. The sinusoidal electric field $E(t)$ can be expressed as a sum of two complex time-varying quantities, $a(t)$ and $a^*(t)$,

$$E(t) = \frac{1}{2}[a(t) + a^*(t)] . \quad (1)$$

These quantities are phasors that rotate in the complex plane as time progresses (see figure 1). A phasor may be described in terms of a complex amplitude a and a

time-dependent factor $e^{-i\omega t}$. The complex amplitude can be represented as $a = x + ip$ where x and p are real. By inverting these relationships, the quadrature components x and p are expressible in terms of a and a^* so that the electric field can be written as

$$E(t) = x \cos \omega t + p \sin \omega t \quad (2)$$

where

$$x = (a + a^*)/2 \quad (3)$$

and

$$p = (a - a^*)/(2i). \quad (4)$$

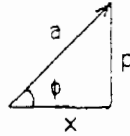


Figure 1. Phasor and quadrature-component representations of the electric field for monochromatic classical light.

The components x and p are called quadrature components because the cosine and the sine differ in phase by 90 degrees, i.e. they are in quadrature. The energy in a classical mode such as this is proportional to the square of the electric field, and therefore to $|a|^2$, which is of course constant and unrestricted in its value.

Assume that at $t = 0$ the phasor $a(t)$ takes on the initial position shown by the broken line a in figure 2. It can then be represented either in terms of its magnitude and initial phase ϕ , or in terms of its initial x and p projections. The phasor rotates with an angular velocity ω , which is the angular frequency of the optical field. Its projection on the x -axis varies sinusoidally with time and has a peak value $|a|$. There are many possible choices of orthogonal coordinate axes, e.g. x' and p' as shown in figure 2.

Single-mode monochromatic light can be represented in an analogous way when viewed from a quantum-mechanical point of view. The quantities $E(t)$, $a(t)$, $a^*(t)$, x , and p in figures 1 and 2 must, however, be converted into operators in a Hilbert space. The laws of quantum mechanics provide that the annihilation operator $a(t)$, and its hermitian conjugate the creation operator $a^\dagger(t)$, obey the boson commutation relation

$$[a(t), a^\dagger(t)] = a(t)a^\dagger(t) - a^\dagger(t)a(t) = 1. \quad (5)$$

This, in turn, means that x and p do not commute with each other. Rather, they obey the commutator

$$[x, p] = \frac{i}{2}. \tag{6}$$

Thus, the quadrature components of the field obey a Heisenberg uncertainty relation of the form

$$\sigma_x \sigma_p \geq \frac{1}{4} \tag{7}$$

where σ represents the standard deviation of the subscripted quantity. Unlike the situation for a classical mode, these components cannot be simultaneously specified with unlimited accuracy. The average energy in the quantum mode is $\hbar\omega(\langle n \rangle + \frac{1}{2})$ where $\hbar\omega$ is the energy per photon and $n = a^\dagger a$ is the photon-number operator. The additional zero-point energy of the field, $\frac{1}{2}\hbar\omega$, represents vacuum fluctuations.

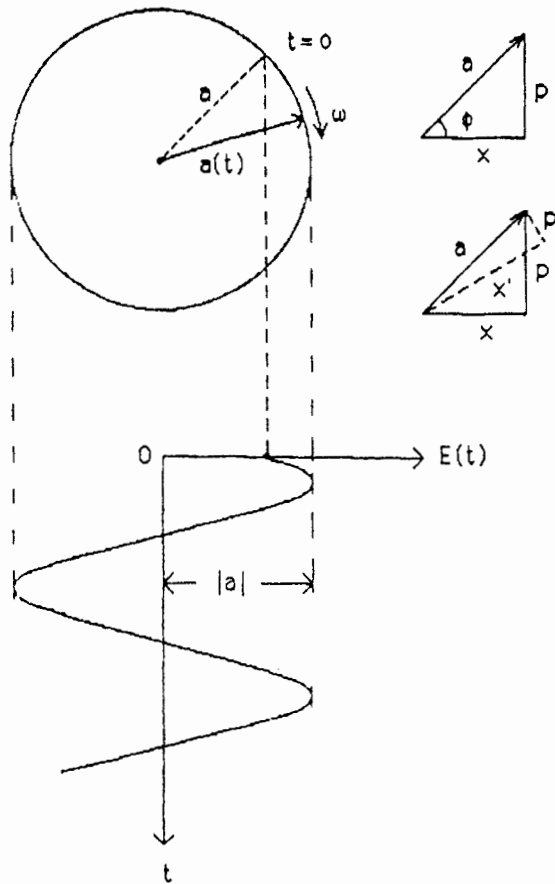


Figure 2. For monochromatic classical light, the selection of different points for $t = 0$ provides different values for x , p and ϕ .

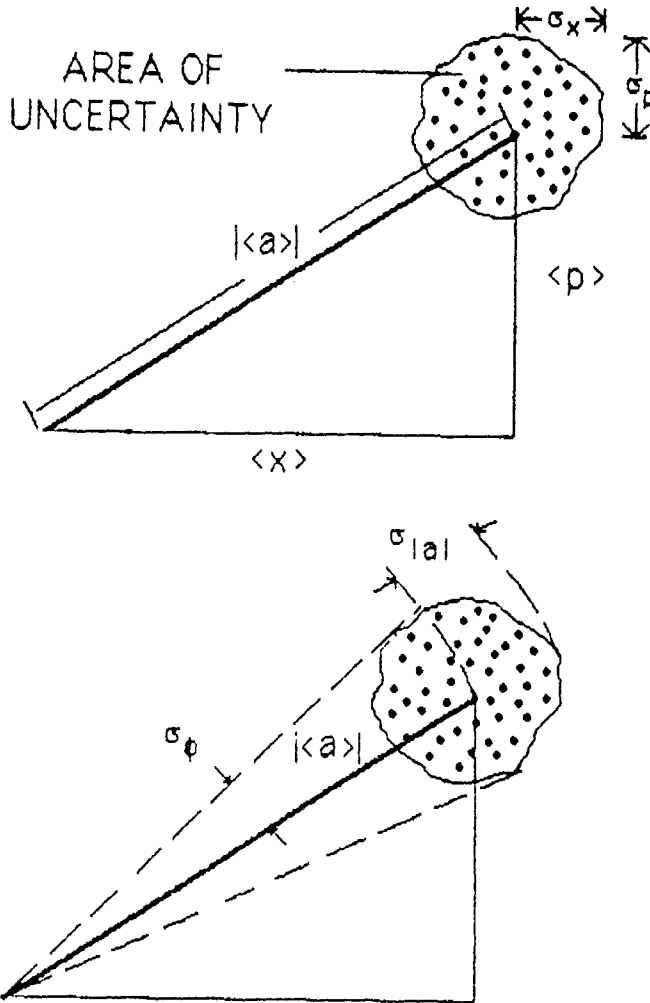


Figure 3. Cartesian and polar-coordinate representations of the uncertainty area associated with a quantum-mechanical field.

The uncertainties associated with each of the quadrature components of this quantum-mechanical field are illustrated in figure 3. The mean values $\langle x \rangle$ and $\langle p \rangle$, and their standard deviations σ_x and σ_p , are shown in the upper portion of the figure. There is an area of uncertainty (dotted region) indicating that the simple classical description of a phasor without randomness does not apply. A state of minimum uncertainty obeys the equality $\sigma_x \sigma_p = \frac{1}{2}$. In the lower portion of figure 3, the uncertainty of a is represented in polar coordinates. It has an amplitude standard deviation $\sigma_{|a|}$, a phase-angle uncertainty σ_ϕ , and a mean magnitude $|a\rangle$. For a sufficiently small area, the photon-number uncertainty σ_n can be written in terms of $\sigma_{|a|}$ by using the approximate relationship $n \approx |a|^2$. Forming the differential

$$\Delta n \approx 2|a|\Delta|a| \tag{8}$$

gives rise to

$$\sigma_n = 2\langle n \rangle^{1/2} \sigma_{|a|} \quad (9)$$

where $\sigma_n \equiv \Delta n$. The azimuthal uncertainty σ_ϕ can be expressed as the ratio of the arc-length uncertainty to $\langle n \rangle^{1/2}$. Although these relationships are not entirely accurate, they nevertheless provide a rough guide to the interrelations of the various uncertainties.

It is clear that both cartesian and polar coordinates provide suitable representations for describing the uncertainties associated with the quantum field. The former turns out to be useful for the analysis of quadrature-squeezed light, and the latter for photon-number-squeezed light, as will soon become evident.

2. Examples of states of light

Two examples of states of light are described in this section. The first is the coherent state [1], which is generated by an ideal amplitude-stabilised gas laser operated well above its threshold of oscillation. As illustrated in the upper portion of figure 4, the coherent state is represented by a phasor of mean magnitude $|\langle a \rangle| = \alpha$ and a surrounding circular area of uncertainty. The probability density $\text{Pr}(x)$ of finding the value x is gaussian, with mean $\langle x \rangle$ and standard deviation $\sigma_x = \frac{1}{2}$. Its quadrature components behave symmetrically so that $\sigma_x \sigma_p = \frac{1}{4}$; the coherent state is a minimum-uncertainty state. The polar-coordinate representation is provided in the lower portion of figure 4. For a coherent state, the photon-number variance σ_n^2 is precisely equal to the photon-number mean, in accordance with the Poisson distribution. Using the expressions for σ_n and σ_ϕ of the previous section, with $\sigma_{|a|} = \frac{1}{2}$ and an azimuthal arc-length uncertainty of $\frac{1}{2}$, leads to the so-called semiclassical number-phase equality

$$\sigma_n \sigma_\phi = \frac{1}{2} . \quad (10)$$

The second example is the vacuum state shown in figure 5. It, too, is a coherent state but with $\alpha = 0$ so that $\langle x \rangle = \langle p \rangle = 0$. It is a minimum-uncertainty state obeying $\sigma_x \sigma_p = \frac{1}{4}$. The vacuum state is also a number state with $n = 0$, as will be discussed subsequently. Although its mean photon number $\langle n \rangle$ is zero, a vacuum-state mode has a zero-point energy $\frac{1}{2}\hbar\omega$ and therefore exhibits residual fluctuations in x , p , and $E(t)$. The vacuum, though devoid of photons, is noisy.

The electric-field time dependence for the coherent state is illustrated in figure 6. Unlike the classical electric field $E(t)$, which has a sharp value at each instant of time (see figure 2), the quantum electric field is always uncertain. This is because a is an operator rather than a complex number. In principle, the gaussian tails of the coherent-state quadrature components allow the amplitude of the coherent field to assume an arbitrarily large value at any instant. However, it will usually be found within one standard deviation (σ) of the mean. Values of α lying in the uncertainty circle (black circle in upper-right quadrant of figure 6) trace out the $\pm\sigma$ limits of $E(t)$ (lower-right quadrant of figure 6), as the circle rotates with angular velocity ω . In the upper- and lower-left quadrants of figure 6 the mechanics of tracing out $E(t)$ from the uncertainty circle is shown for four arbitrarily chosen values of α in the uncertainty circle. Each value of α traces out a sinusoidal time function, of appropriate magnitude and phase,

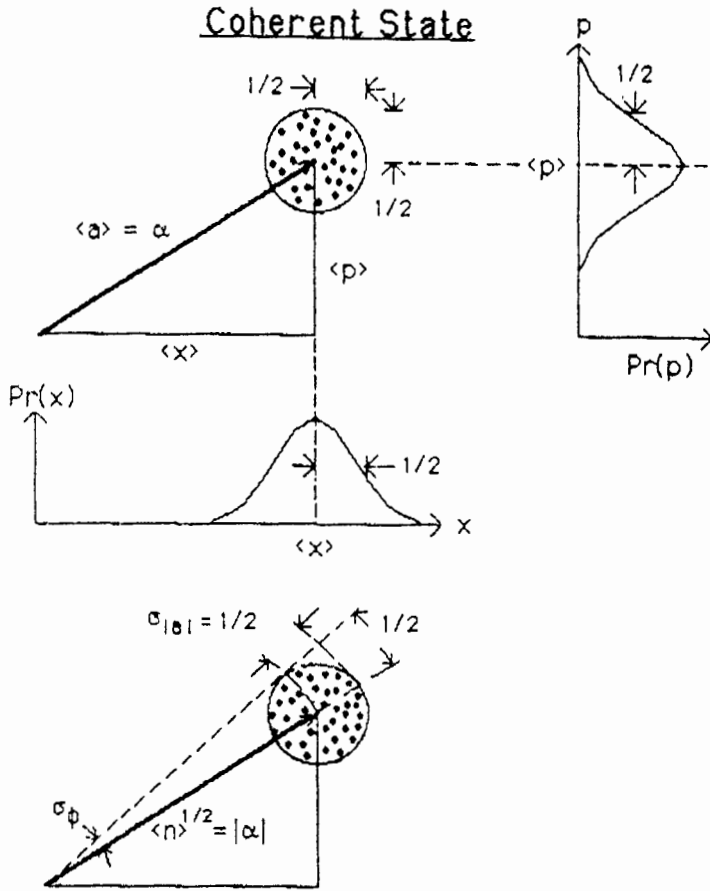


Figure 4. Quadrature-component and number-phase uncertainties for the coherent state.

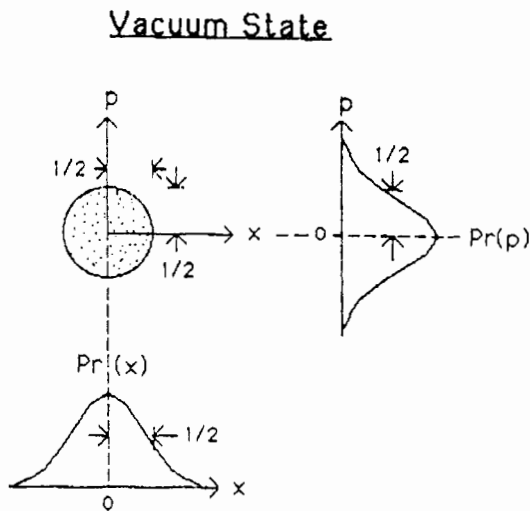


Figure 5. Quadrature-component uncertainties for the vacuum state.

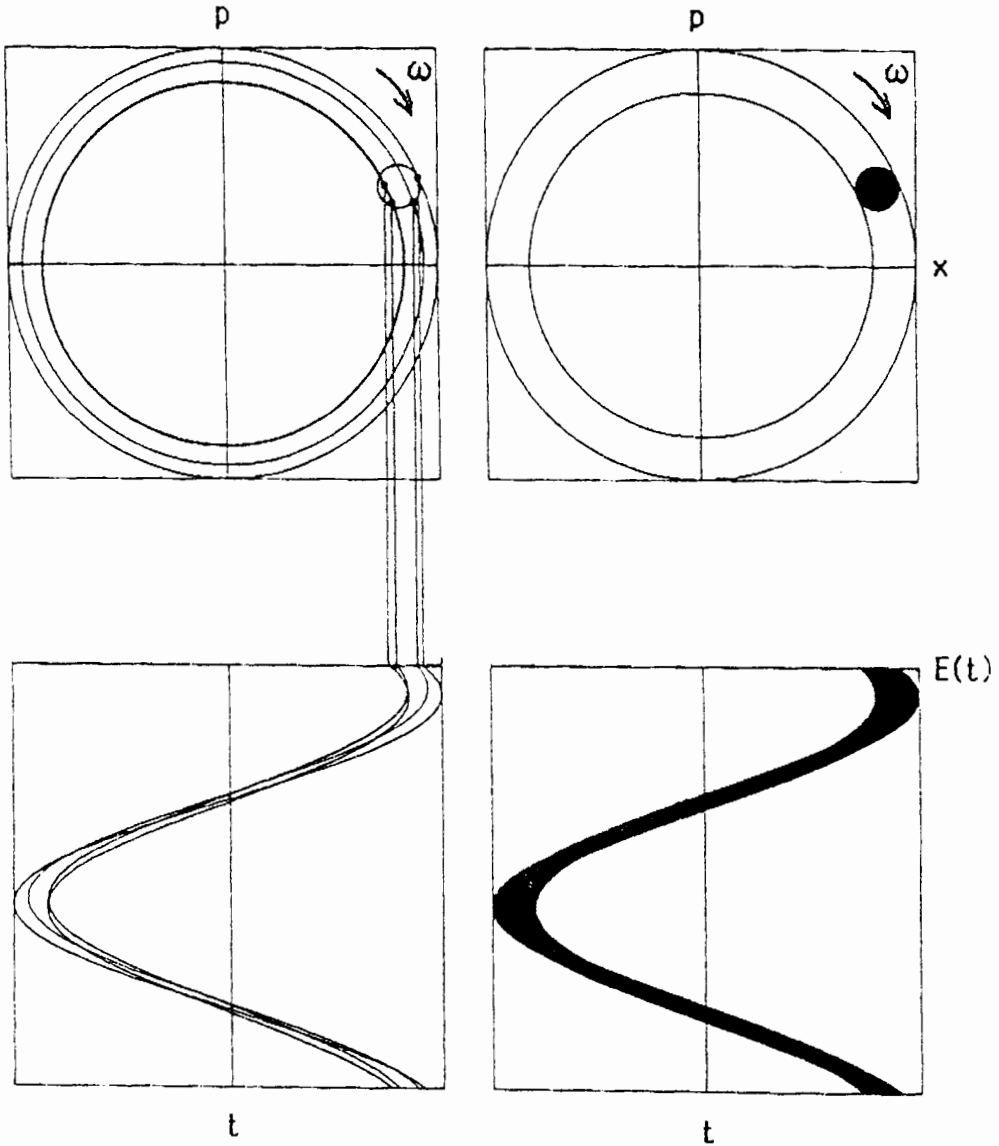


Figure 6. Electric-field time dependence for the coherent state.

as determined by its real part (projection on the x-axis). The collection of all points within the uncertainty circle produces $E(t)$ as shown in the lower-right quadrant. For the coherent state, the noise about the mean of the electric field is independent of its phase.

The behaviour of the electric-field time dependence for the vacuum state is obtained in the same way, as illustrated in figure 7. The sinusoidal time functions traced out by six possible values of α falling within the uncertainty circle are shown in the upper- and lower-left quadrants. The collection of all points within the circle traces out the $\pm\sigma$ limits of $E(t)$. Although it is noisy, the mean of the vacuum-state field is, of course, zero. Again, the noise is phase-independent.

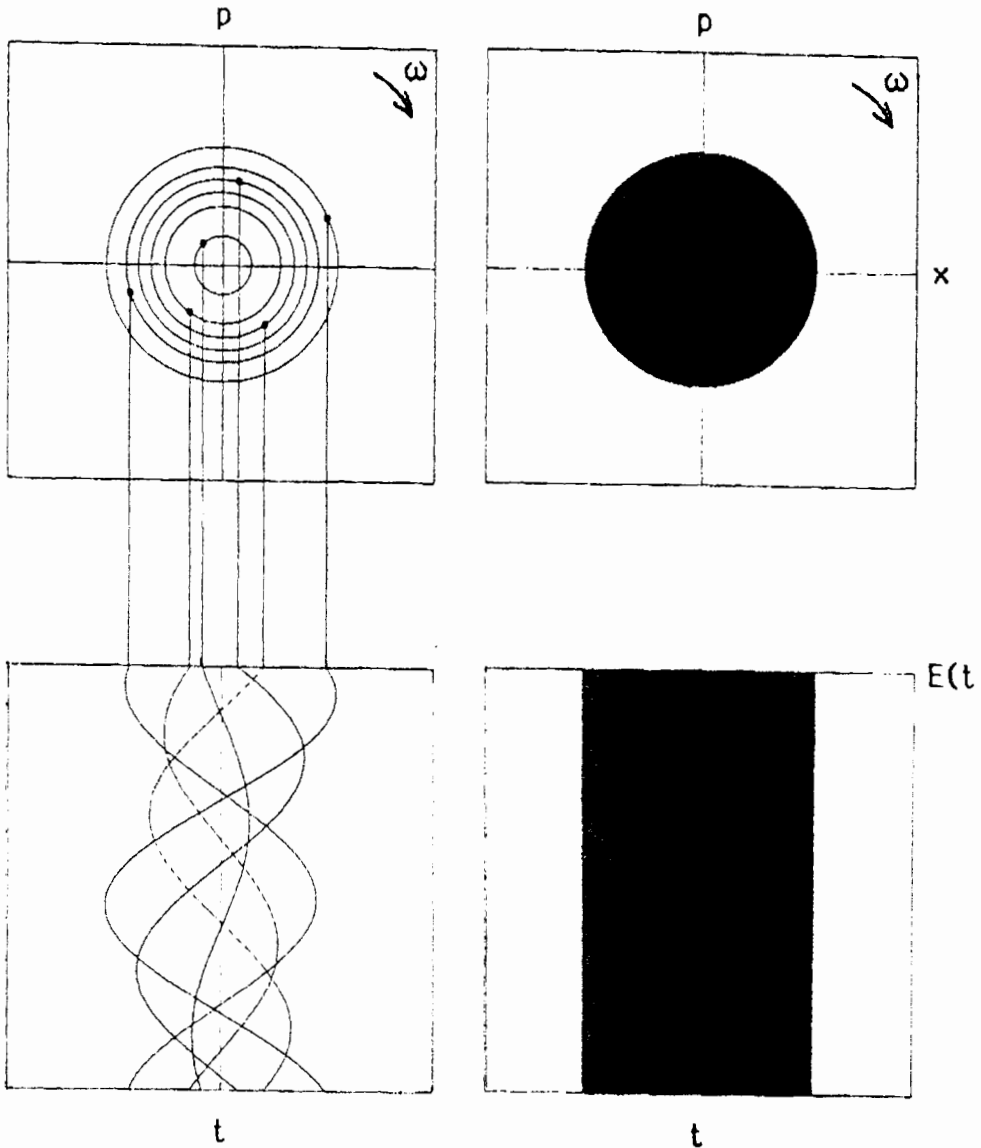


Figure 7. Electric-field time dependence for the vacuum state.

3. Definitions of squeezed-state light

The coherent and vacuum states described above are not squeezed. We now consider two kinds of squeezed states.

A state is *quadrature-squeezed*, by definition, if any of its quadratures has a standard deviation that falls below the coherent-state (or vacuum-state) value of $\frac{1}{2}$ [2–10]. The uncertainty in one quadrature may be squeezed below $\frac{1}{2}$, but this is achievable only at the expense of stretching the uncertainty in the other quadrature to

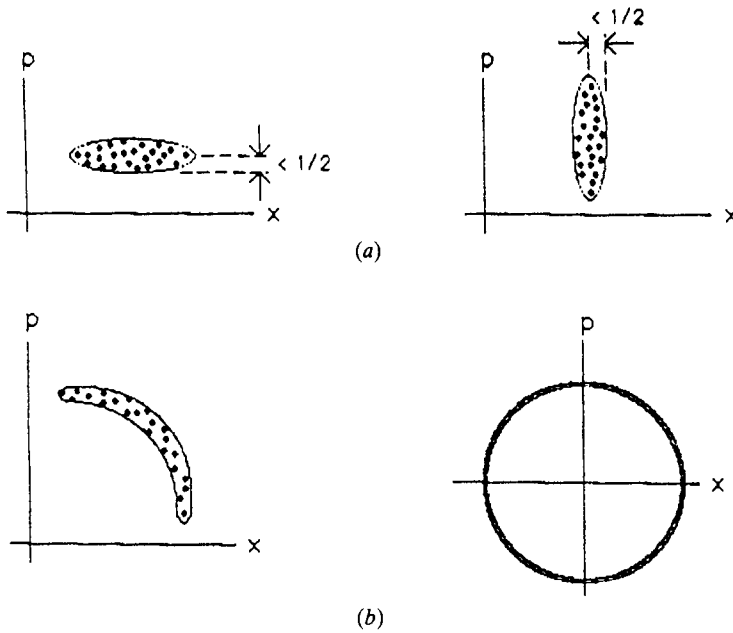


Figure 8. Definitions of squeezed-state light: (a) quadrature squeezed, (b) photon-number squeezed.

a value above $\frac{1}{2}$, as illustrated in the upper portion of figure 8. The product must have a value of $\frac{1}{4}$ or greater, as specified by the Heisenberg uncertainty principle. A quadrature-squeezed state may, but need not, be a minimum-uncertainty state.

In contrast, a state is defined to be *photon-number-squeezed* if its photon-number uncertainty σ_n falls below that of the coherent state, $\langle n \rangle^{1/2}$ [11–15]. The σ_n is related to the radial uncertainty $\sigma_{|a|}$ (see figure 3). The uncertainty in n may be squeezed below $\langle n \rangle^{1/2}$, but only at the expense of stretching the phase uncertainty σ_ϕ , as illustrated in the lower portion of figure 8. Photon-number-squeezed light goes by a number of other names; these include sub-Poisson light, quiet light, silent light, and amplitude-squeezed light (which is also used to refer to a particular kind of quadrature-squeezed light). It is often referred to as sub-Poisson light because its standard deviation falls below (sub) that of the Poisson distribution that characterises the coherent state. A photon-number-squeezed state need not obey the minimum-uncertainty number-phase equality $\sigma_n \sigma_\phi = \frac{1}{2}$, although states that do obey this relation have been studied [16].

4. Examples of quadrature-squeezed light

From a mathematical point of view, a field in a minimum uncertainty state can be quadrature squeezed by multiplying its x -component by the factor e^{-r} and its p -component by the factor e^r . The quantity r is called the ‘squeeze parameter’. It is convenient to include a phase factor $e^{i\theta}$ in one of the quadratures so that

$$E_s(t) = xe^{-r}e^{i\theta} \cos \omega t + pe^r \sin \omega t . \tag{11}$$

The net result of this operation is to squeeze the x -component uncertainty σ_x down to $e^{-r}\sigma_x$ and simultaneously to stretch the p -component uncertainty σ_p up to $e^r\sigma_p$. As illustrated in figure 9, the vacuum state then becomes the squeezed vacuum state. Both are minimum-uncertainty states. Note, however, that the squeezed vacuum state has a mean photon number

$$\langle n \rangle = \sinh^2 r > 0 \tag{12}$$

so that it no longer truly represents a vacuum. Furthermore its photon-number statistics are super-Poisson; its variance

$$\sigma_n^2 = 2(\langle n \rangle + \langle n \rangle^2) \tag{13}$$

is twice that of the Bose-Einstein (geometric) distribution.

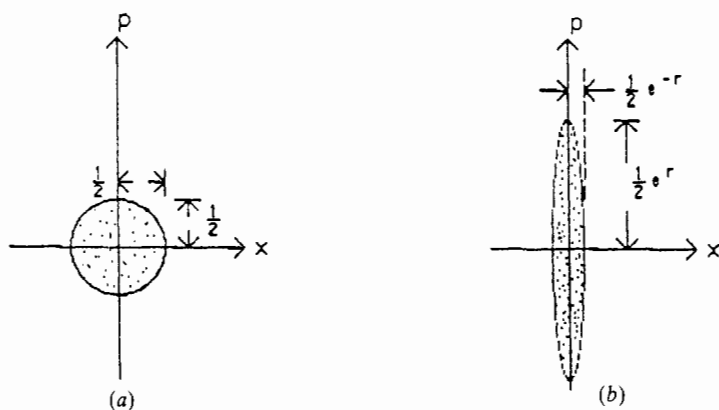


Figure 9. Comparison of quadrature-component uncertainties for the vacuum and squeezed vacuum states: (a) vacuum state, (b) squeezed vacuum state.

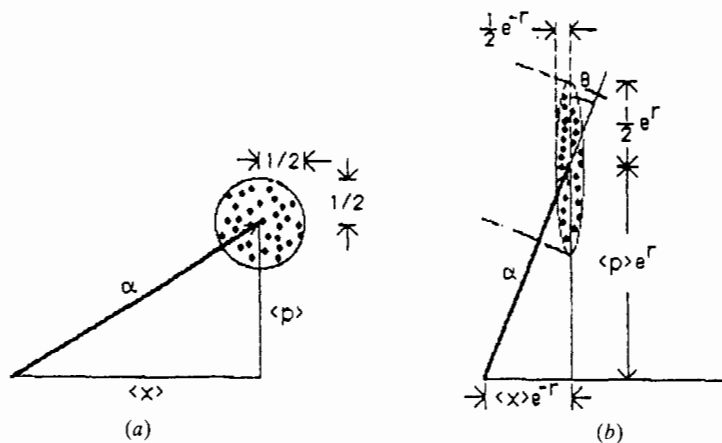


Figure 10. Comparison of quadrature-component uncertainties for the coherent and squeezed coherent states: (a) coherent state, (b) squeezed coherent state.

The coherent state can be similarly transformed into the squeezed coherent state, as shown in figure 10. This minimum-uncertainty state goes by a number of other names [2], including the ‘two-photon coherent state’, the ‘wave-packet state’, and the ‘new coherent state’. The angle θ between the major axis of the ellipse and the phasor $\alpha = \langle a \rangle$ is controlled by changing the angle ξ relative to the angle of α . The mean photon number

$$\langle n \rangle = |\alpha|^2 + \sinh^2 r \tag{14}$$

has both a coherent contribution $|\alpha|^2$ and a squeeze contribution $\sinh^2 r$. Its variance is

$$\sigma_n^2 = \langle n \rangle (e^{2r} \cos^2 \theta + e^{-2r} \sin^2 \theta), \quad |\alpha|^2 \gg e^{2r}. \tag{15}$$

The squeezed coherent state can exhibit either super-Poisson or sub-Poisson photon statistics, depending on the angle θ , as shown in figure 11 for the example $r = \frac{1}{2}$. The variance is largest when θ is an even integer multiple of $\pi/2$. Referring back to figure 10, this corresponds to the major axis of the ellipse aligning with the phasor. This lends a large uncertainty to the radial direction, thereby giving rise to a large photon-number variance. In contrast, the photon-number variance is smallest when θ is an odd integer multiple of $\pi/2$. In this case the minor axis of the ellipse lends a small uncertainty to the radial direction and thereby to the photon-number variance.

The electric-field time dependences for the squeezed vacuum state and the squeezed coherent state are shown in figures 12 and 13, respectively. Diagrams of this kind were first presented by Caves [17]. In these illustrations the p -components are taken to be squeezed, rather than the x -components, as in figures 9 and 10. The former is sometimes referred to as phase squeezing and the latter as amplitude squeezing. The electric-field uncertainty is seen to fall to a minimum periodically; the noise is reduced below the coherent-state value at certain preferred values of the

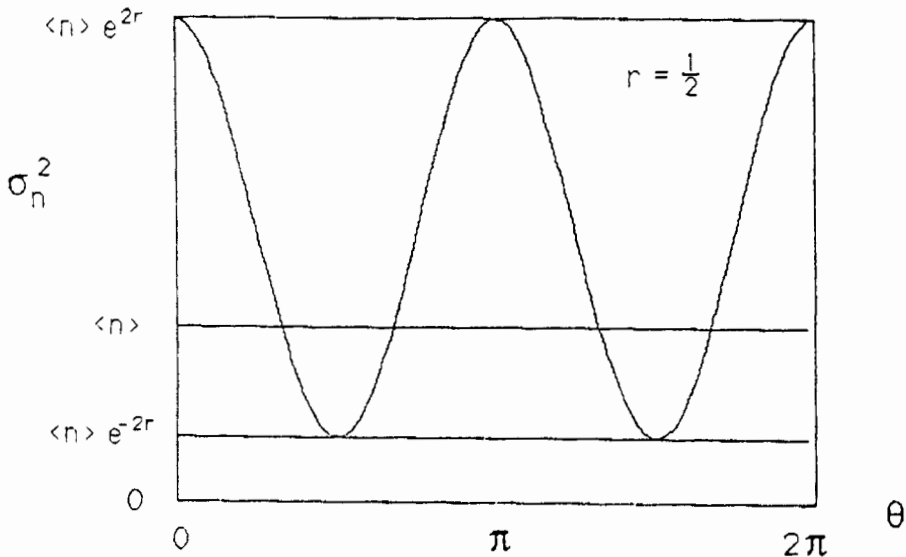


Figure 11. Dependence of the squeezed coherent state photon-number variance, σ_n^2 , on the angle θ . The light is super- or sub-Poisson depending on θ .

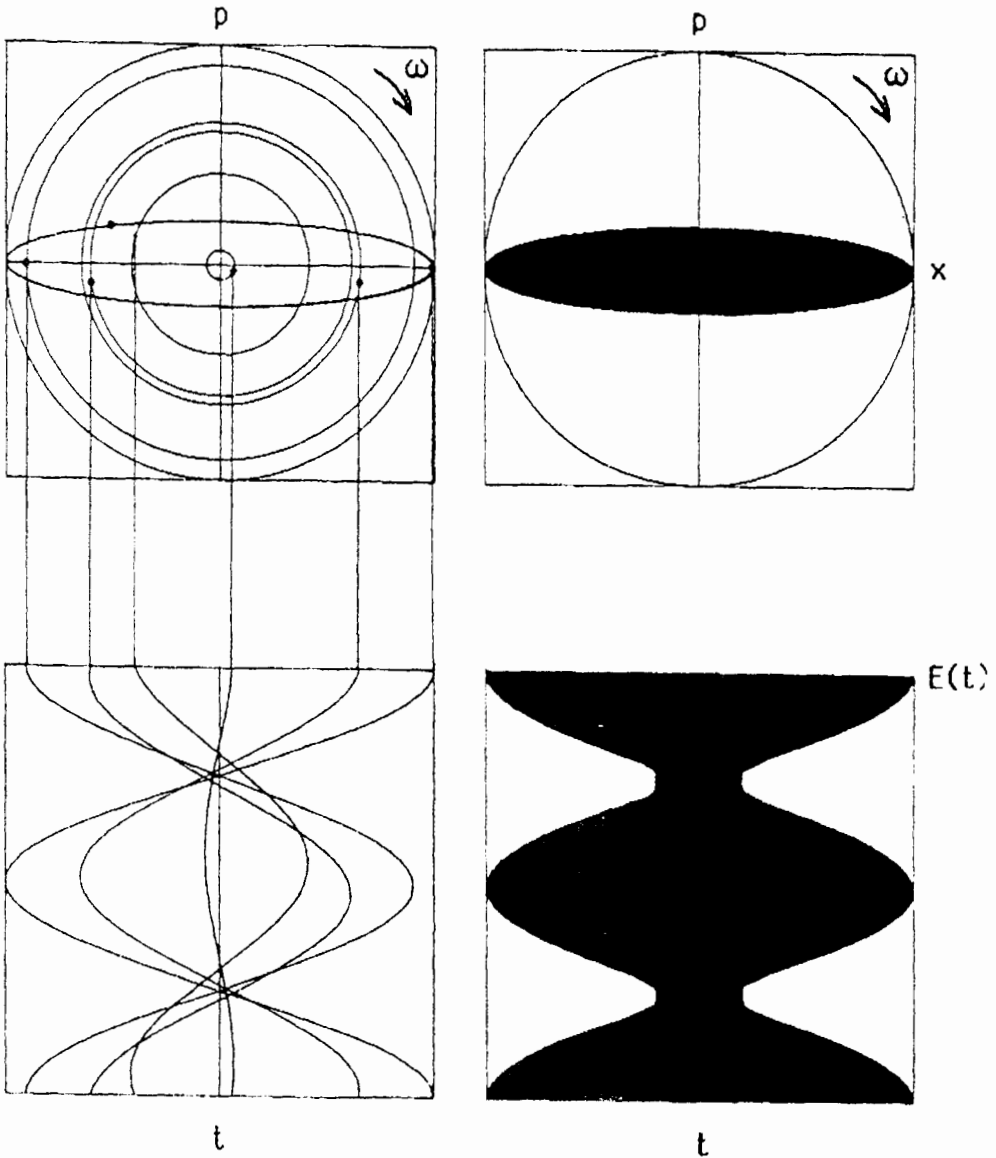


Figure 12. Electric-field time dependence for the squeezed vacuum state.

phase. This benefit, of course, comes at the expense of an increase in the noise at other values of the phase. In contrast, the noise of unsqueezed states, such as the vacuum state (figure 7) and the coherent state (figure 6), is the same for all values of the phase.

As a final example, illustrated in figure 14, we consider the superposition of a vacuum field, a_v , and a coherent field, a_c , by the use of a 50/50 lossless beamsplitter. This device has an intensity transmission coefficient $\eta = \frac{1}{2}$ and a field transmittance $\sqrt{\eta} = 1/\sqrt{2}$. The means and variances of the superposed quadrature field components are taken to be the sums of the individual contributions at the output port:

$$\langle x \rangle = \frac{\langle x_c \rangle}{\sqrt{2}} + 0 \tag{16}$$

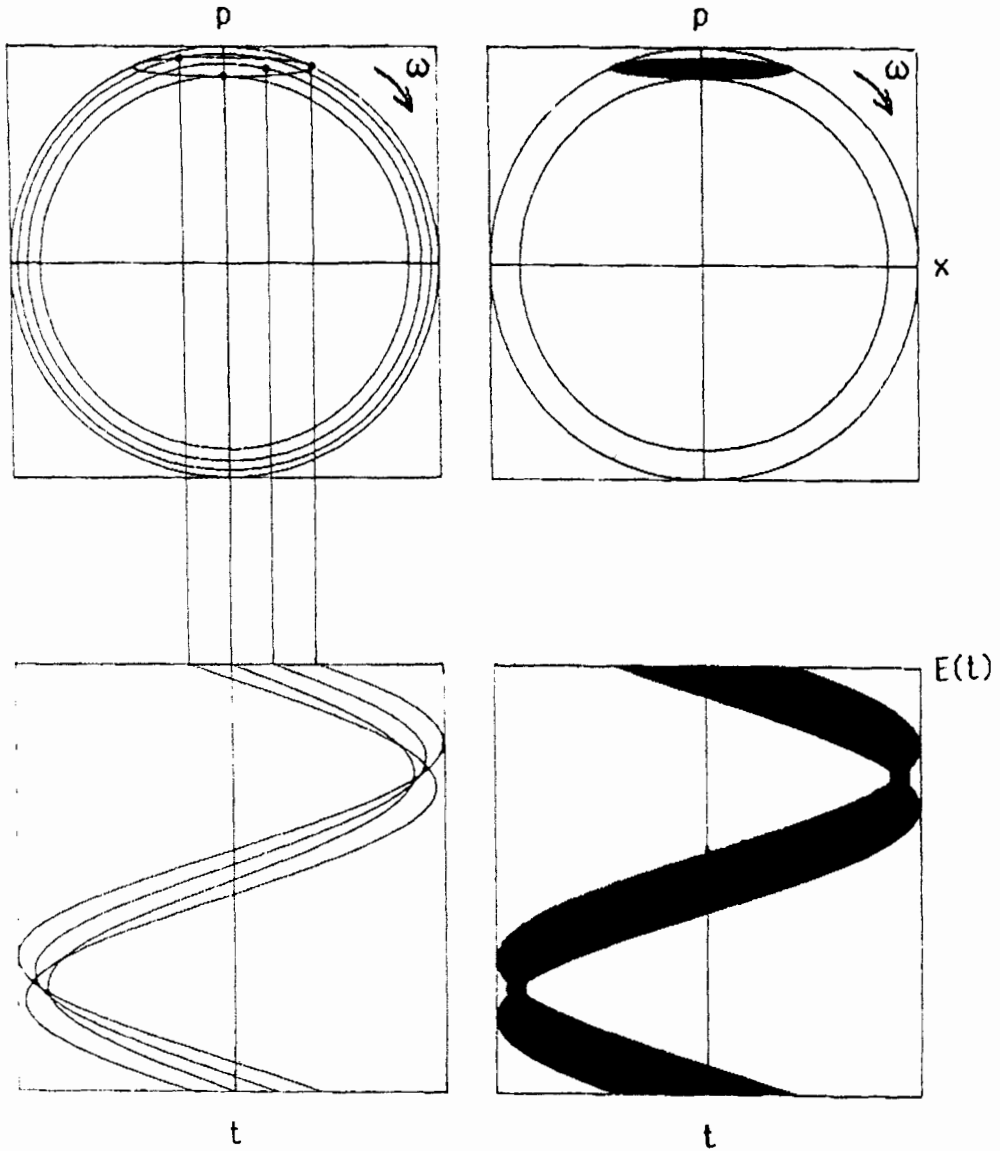


Figure 13. Electric-field time dependence for the squeezed coherent state.

$$\langle p \rangle = \frac{\langle p_c \rangle}{\sqrt{2}} + 0 \tag{17}$$

$$\sigma_x^2 = \frac{\sigma_{xc}^2}{2} + \frac{\sigma_{xv}^2}{2} \tag{18}$$

$$\sigma_p^2 = \frac{\sigma_{pc}^2}{2} + \frac{\sigma_{pv}^2}{2} . \tag{19}$$

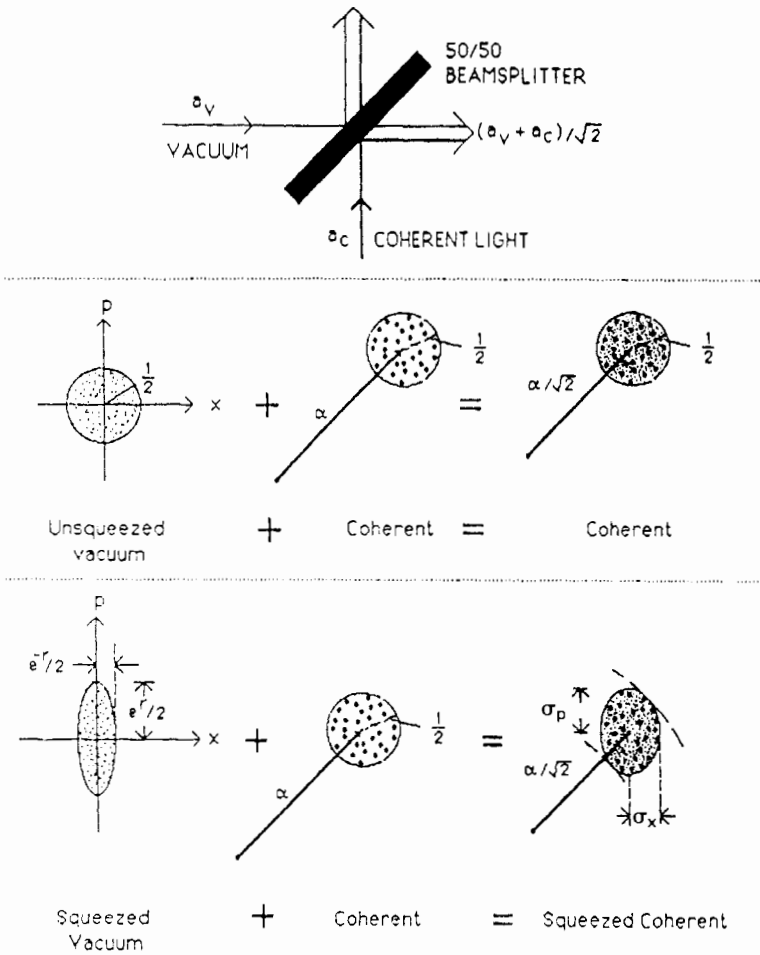


Figure 14. Quadrature-component uncertainties for the superposition of a coherent field with unsqueezed and squeezed vacuum fields at a 50/50 beamsplitter.

Using this rule, an unsqueezed vacuum field superposes with coherent light to produce coherent light of reduced mean. This is the expected result since unsqueezed vacuum simply represents an open port. On the other hand, a squeezed vacuum field superposed with coherent light leads to a squeezed field with properties intermediate between the squeezed vacuum and the unsqueezed coherent field with

$$\sigma_x = \frac{1}{2} \sqrt{\frac{(1 + e^{-2r})}{2}} < \frac{1}{2} \tag{20}$$

and

$$\sigma_p = \frac{1}{2} \sqrt{\frac{(1 + e^{2r})}{2}} > \frac{1}{2}. \tag{21}$$

The squeezing properties of the superposition can be enhanced by using an unequal beamsplitter ($\eta > \frac{1}{2}$). We then have an output field

$$a - \sqrt{\eta} a_v + \sqrt{1 - \eta} a_c. \quad (22)$$

As $\eta \rightarrow 1$, ($1 - \eta \rightarrow 0$), with $(1 - \eta)|\alpha|^2 \gg \frac{1}{2}$, the superposition becomes as fully squeezed as the squeezed vacuum. However, this requires that $|\alpha|^2 \rightarrow \infty$, i.e. that the coherent field be arbitrarily strong.

5. Detection of quadrature-squeezed light

Several methods can be considered for the detection of quadrature-squeezed light: direct detection, single-ended homodyne detection, and balanced homodyne detection. Direct detection records the photon counts. The squeezed vacuum state has a mean photon number and a photon-number variance given by equations (12) and (13) above. This state has twice the Bose–Einstein variance, i.e. it is highly super-Poisson and therefore noisy. Direct detection is not generally suitable for detecting quadrature-squeezed light because it fails to discriminate against the noisy quadrature. Because there are certain values of the phase where the electric field variability becomes small, however, we turn instead to a phase-sensitive form of detection, viz. homodyning [4].

Homodyning can be used to extract the quadrature of the field with reduced fluctuations. In the single-ended configuration (figure 14), the squeezed-vacuum light is combined at an unequal beamsplitter with the coherent light, a_c , from a laser local oscillator (LO). If $\eta \rightarrow 1$, with a sufficiently strong LO, the superposition field shares characteristics with the squeezed coherent state. If the LO phase is chosen properly, so that θ is an odd integral multiple of $\pi/2$ (see figures 10 and 11), the superposition field will be photon-number squeezed, resulting in sub-Poisson photocounts or, equivalently, a sub-shot-noise spectrum.

A problem with single-ended homodyne detection is that a very strong local oscillator is required to achieve the optimal conditions. Furthermore, unwanted (but sometimes unavoidable) fluctuations in the power of the local oscillator (excess noise) serves to increase the noise in the superposition beam, and therefore to mask the squeezing. A few years ago Yuen and Chan [18] suggested a modification of the single-ended configuration based on the ideas of balanced detection in microwave mixers and optical systems [19]. This method has important implications for eliminating the quantum noise in the coherent local oscillator, as well as excess LO noise, as shown in figure 15. A squeezed vacuum signal and a coherent local oscillator are incident on a 50/50 beamsplitter. The light in both output ports is detected so that no energy is lost. Because of the phase shift at the beamsplitter, the contributions of the vacuum at the output ports differ by a sign. After the two beams are detected, they are differenced to provide the balanced-detector output.

The process can be described in terms of the diagrams shown at the bottom of figure 15. The lines and circles represent the coherent state; the ellipses represent the squeezed vacuum state. The uncertainties arising from the coherent-state LO appear at both output ports; because they are correlated they can be subtracted. In contrast, the uncertainties associated with the squeezed vacuum states are anticorrelated and therefore add when subtracted. The net result is that the original squeezed vacuum

uncertainty is recovered with no quantum or excess noise contributed by the local oscillator. This is an important result because it shows that the balanced mixer can be effectively used to achieve ideal homodyne detection.

6. Generation of quadrature-squeezed light

Quadrature-squeezed light may be generated by separating the field into its x and p components, and then by stretching one and squeezing the other. To accomplish the separation, a phase shift must be introduced. A nonlinear optical medium that provides phase conjugation can achieve this, as illustrated in figure 16. If the wave and its conjugate are multiplied by $\mu = \cosh r$ and $\nu = \sinh r$, respectively, and then added, the net result is a quadrature-squeezed field with squeeze parameter r . Due to the trigonometric relation between $\cosh r$ and $\sinh r$

$$\mu^2 - \nu^2 = 1 . \tag{23}$$

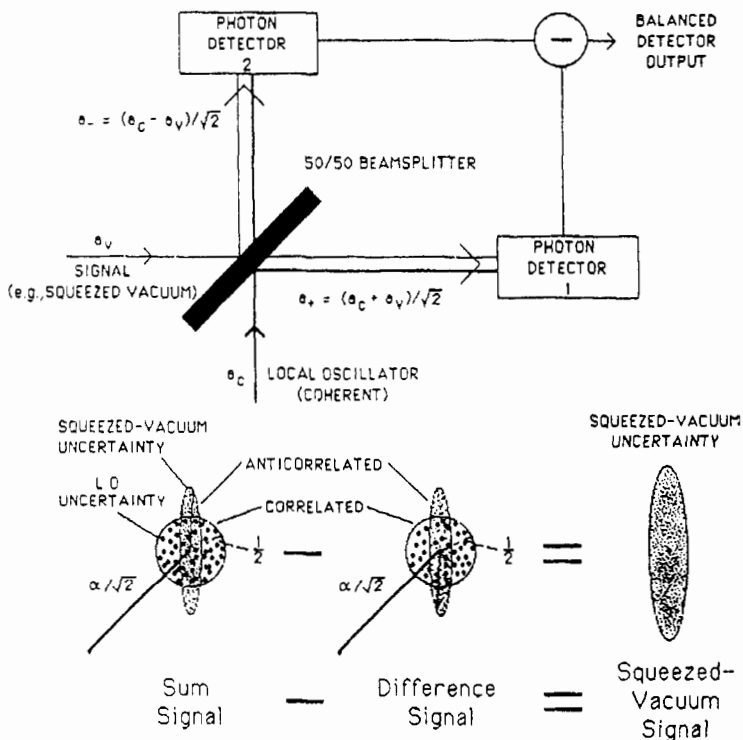


Figure 15. Balanced homodyne detection of a squeezed vacuum field.

Since the wave is stretched by $\cosh r$, and its conjugate by $\sinh r$, the superposition may be viewed schematically as in figure 17.

Yuen and Shapiro [20] were the first to consider the generation of quadrature-squeezed light by the use of a phase-conjugate mirror. They suggested implementing the process by degenerate four-wave mixing, as indicated schematically in figure 18. A phase-conjugate mirror of this type multiplies by a constant and conjugates fields reflected from it ($a \rightarrow \nu a^\dagger$), but simply multiplies transmitted fields by a constant ($a \rightarrow \mu a$). Any open port in such a system admits vacuum fluctuations that can serve to reduce the squeezing. In the phase-conjugate mirror, however, the vacuum fluctuations are converted to squeezed vacuum fluctuations which do not dilute the squeezing properties of the result, which is the squeezed coherent state.

Quadrature-squeezed light has been generated nearly simultaneously by Slusher *et al* [21] and in a number of other laboratories, using a variety of three- and four-wave mixing schemes [22–25]. Substantial noise reduction (below the shot-noise level) has been achieved, most notably in the experiments of Kimble and his co-workers [23, 26].

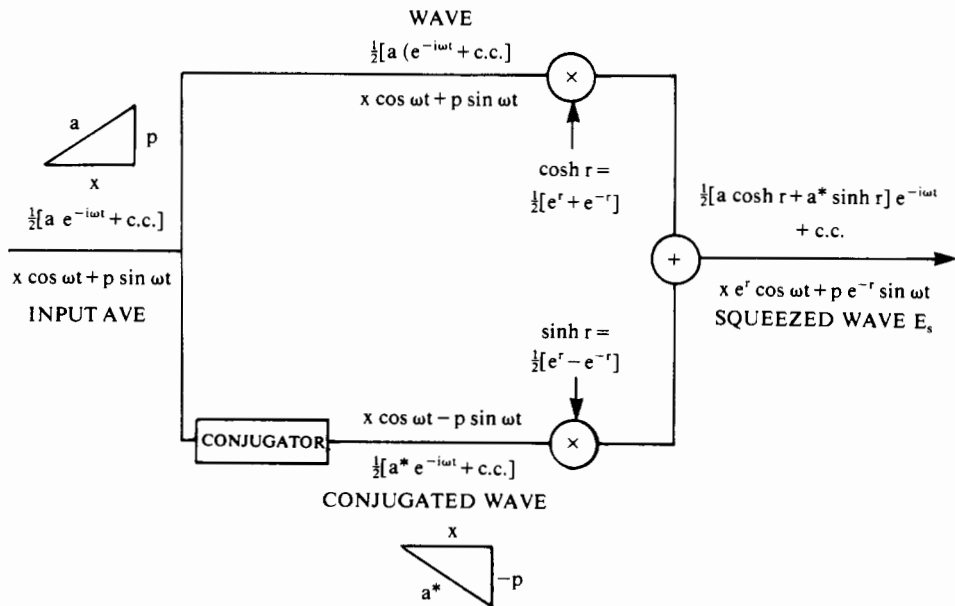


Figure 16. Generation of quadrature-squeezed light by the use of a nonlinear medium providing phase conjugation.

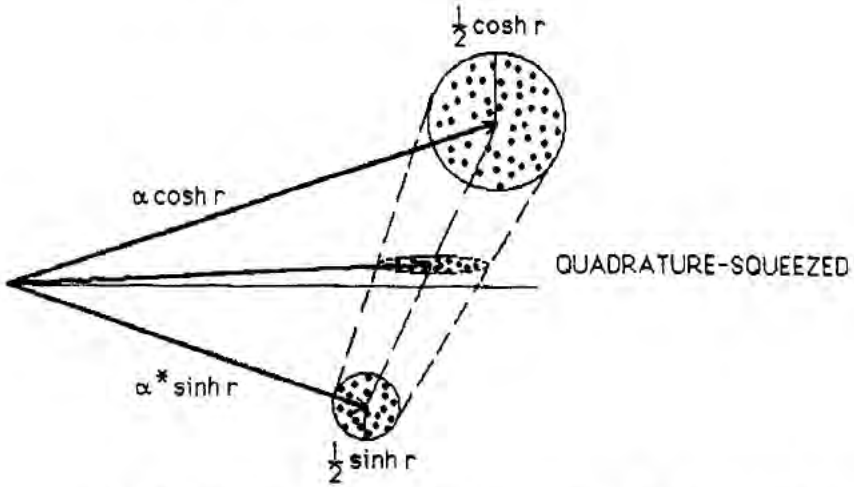


Figure 17. Schematic illustration of quadrature-squeezed light generation using phase conjugation.

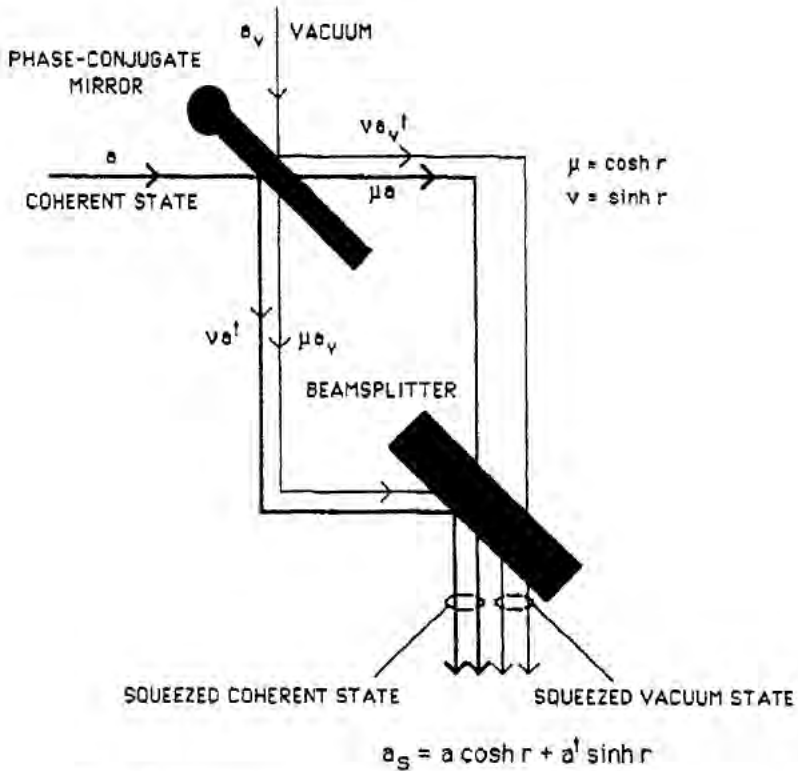


Figure 18. Generation of quadrature-squeezed light using a phase-conjugate mirror (implemented by degenerate four-wave mixing).

7. Examples of photon-number-squeezed light

We turn now to photon-number squeezing. A principal example is provided by the number (Fock) state depicted in figure 19 [27]. It has the properties

$$\sigma_x = \left(\frac{n}{2} + \frac{1}{4}\right)^{1/2}; \quad \sigma_p = \left(\frac{n}{2} + \frac{1}{4}\right)^{1/2} \tag{24}$$

$$\sigma_{|a|} \approx 1; \quad \sigma_\phi = \infty \tag{25}$$

$$\sigma_{|a|}/\langle a \rangle = \langle n \rangle^{-1/2} \tag{26}$$

$$\sigma_n = 0. \tag{27}$$

Its quadrature uncertainties are symmetrical and large; it is not a minimum-uncertainty state. In the polar-coordinate representation, its phase is totally uncertain though its magnitude (represented by the radial uncertainty) is rather restricted. According to quantum mechanics, however, the mean photon number $\langle n \rangle$ has a variability σ_n that is precisely zero for the number state. This state is therefore squeezed in its photon number, since $\sigma_n < \langle n \rangle^{1/2}$ (see §3), rather than in one of its quadratures, x or p . The number state represents a nonclassical field, not by virtue of its phase properties, but rather by virtue of its amplitude properties.

The electric-field time dependence for the number state is illustrated in figure 20. Phasors within the uncertainty area trace out an electric field of rather constant amplitude but of uniformly distributed phase. However its photon number is deterministic. For $n = 0$, the number state is to be distinguished from the vacuum state (figure 7) where the phasor magnitude is arbitrary. The $n = 0$ number state is the vacuum state, as is the $\alpha = 0$ coherent state.

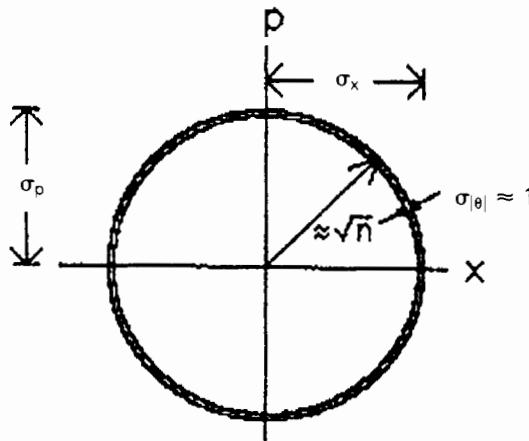


Figure 19. Quadrature-component and number-phase uncertainties for the number state.

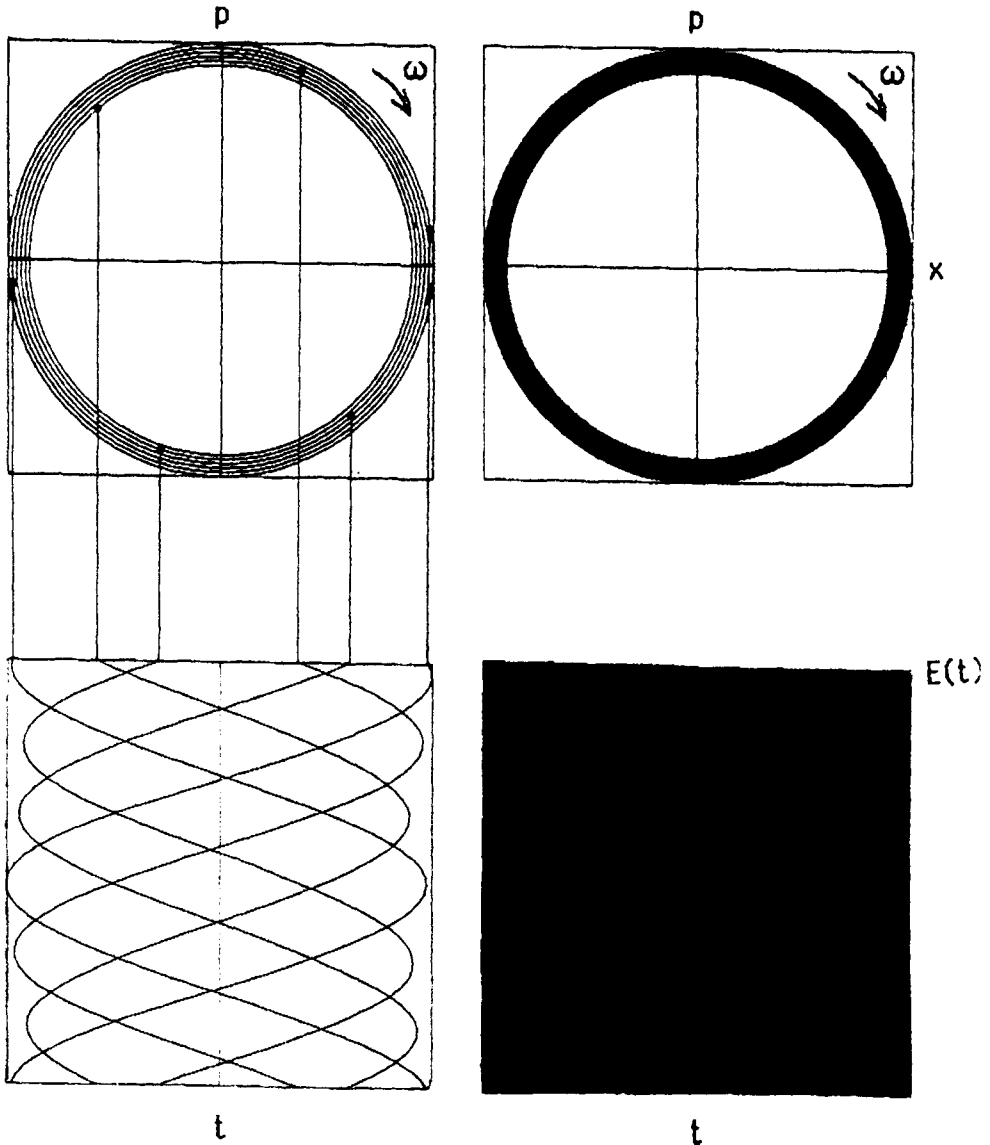


Figure 20. Electric-field time dependence for the number state.

8. Detection of photon-number-squeezed light

In contrast with quadrature-squeezed light where homodyning is useful for detection, photon-number-squeezed light may be observed with direct detection [15]. Two photon-counting approaches to direct detection are illustrated in figure 21. The photoelectron point process (figure 21(a)) is a time record of the photons registered by the detector. When generated by photon-number-squeezed light it has a distinct character; in the counting time T the photon-number variance σ_n^2 is less than the photon-number mean $\langle n \rangle$. The photon registrations are sub-Poisson. The Fano factor

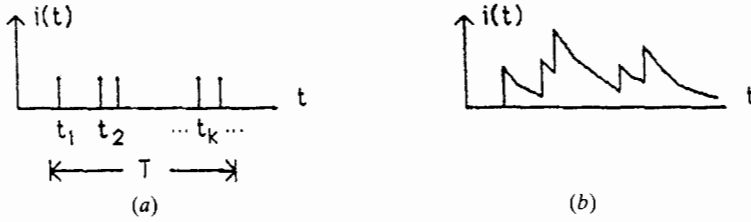


Figure 21. Direct detection of photon-number-squeezed light: (a) photoelectron point process, (b) filtered photoelectron point process.

$$F_n = \sigma_n^2 / \langle n \rangle \tag{28}$$

i.e., the variance divided by the mean, is therefore less than unity. A Poisson distribution, such as that generated by coherent light, has a variance that is always identically equal to the mean and thus a Fano factor of unity. A super-Poisson distribution, by definition, has a Fano factor greater than unity.

If the photoelectron point process is detected in filtered form, the result is illustrated in figure 21(b). In this case, the variables of interest are the mean current

$$\langle i \rangle = \frac{e \langle n \rangle}{T} = 2eB \langle n \rangle \tag{29}$$

where e is the electronic charge, the current variance

$$\sigma_i^2 = (2eB)^2 \sigma_n^2 \tag{30}$$

and the detection filter bandwidth $B (= 1/2T)$. The role of the Fano factor F_n is played by $\sigma_i^2 / 2e \langle i \rangle B$. Photon-number-squeezed light therefore produces a sub-shot-noise photocurrent with

$$\frac{\sigma_i^2}{2e \langle i \rangle B} < 1 \tag{31}$$

or, if the point process is observed in unfiltered form, sub-Poisson photon counts ($F_n < 1$).

9. Generation of photon-number-squeezed light

Photon-number-squeezed light may be generated by introducing anticorrelations into successive photon occurrences [15]. One way to visualise this is by means of an analogy with a photon gun, as illustrated in figure 22. Photon guns naturally generate random (Poisson) streams of photons (figure 22(a)). The production of photon-number-squeezed light can be achieved in three ways: by regulating the times at which the trigger is pulled, by introducing constraints into the firing mechanism, and/or by selectively deleting some of the Poisson bullets after they are fired. Each of these techniques involves the introduction of anticorrelations, which results in a more

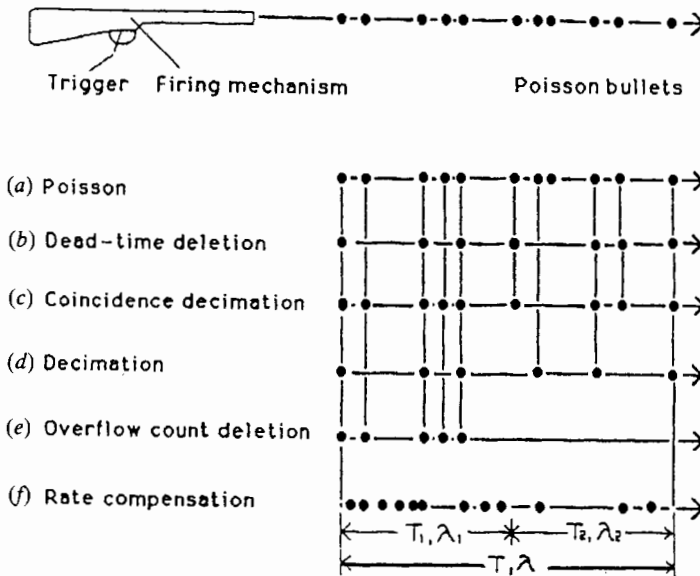


Figure 22. Schematic representation of three components of a simple photon-generation system. A trigger process excites a photon emitter (firing mechanism), which in turn emits photons (Poisson bullets). Anticorrelations can be induced in any of the three elements (from [15], reprinted with permission from North-Holland publishing.).

predictable sequence of events. The anticorrelations themselves are introduced by means of a feedback (or feedforward) process of one kind or another.

Several specific schemes for introducing such photon anticorrelations are shown in figure 22. Dead-time deletion (figure 22(b)) prohibits photons from being arbitrarily close to each other. This effect can result from a requirement that the trigger or firing mechanisms reset between consecutive shots. This is, in fact, the way in which isolated atoms behave in the course of emitting resonance fluorescence photons [11, 28, 29]. Under appropriate conditions, dead time can instead be imposed on the bullets after they are fired. The dead-time deletion process regularises the events, as is apparent from the figure, thereby reducing the randomness of the number of events registered in the fixed counting time T .

Photon anticorrelations can also be introduced by coincidence decimation, which is a process in which closely spaced pairs of photons are removed from the stream (figure 22(c)). Optical second-harmonic generation (SHG), for example, is a nonlinear process in which two photons are exchanged for a third photon at twice the frequency. Both photons must be present within the intermediate-state lifetime of the SHG process for the nonlinear photon interaction to occur. Again, the removal of closely spaced pairs of events regularises the photon stream.

The process of decimation is defined as every N th photon ($N = 2, 3, \dots$) of an initially Poisson photon stream being passed while all intermediate photons are deleted. The passage of every other photon ($N = 2$) is explicitly illustrated in figure 22(d). The regularisation effect on the photon stream is similar to that imposed by dead-time deletion. This mechanism can be used when sequences of correlated photon pairs are emitted; one member of the pair can be detected and used to operate a gate that selectively passes every N th companion photon.

Overflow count deletion is another feedback mechanism that can introduce anti-correlations (figure 22(e)). The number of photons is counted in a set of preselected time intervals $[0, T]$, $[T, 2T]$, ...; the first n_0 photons in each interval are retained and the remainder deleted. If the average number of photons in $[0, T]$ of the initial process is much greater than n_0 , then the transformed process will almost always contain n_0 counts per time interval.

Finally, rate compensation is illustrated in figure 22(f). In this case the (random) number of photons is counted in a short time T_1 ; this information is fed back to control the future rate at which the trigger is pulled. If the random number measured in T_1 happens to be below average, the trigger is subsequently pulled at a greater rate and vice versa. More generally, each photon registration at time t_i of a hypothetical Poisson photon process of rate δ_0 causes the rate λ of the transformed point process to be modulated by the factor $h(t - t_i)$ (which vanishes for $t < t_i$). In linear negative feedback the rate of the transformed process becomes

$$\mu_t = \lambda_0 - \sum_i h(t - t_i) . \quad (32)$$

A variety of techniques can be used to implement rate compensation, such as quantum nondemolition (QND) measurements or correlated photon pairs. Dead-time deletion can be viewed as a special case of rate compensation in which the occurrence of each event sets the rate of the process to zero for a specified period of (dead) time after the registration.

We first consider the generation of *conditionally* photon-number-squeezed light (figure 23). This effect can only be observed by gating the detector open for a

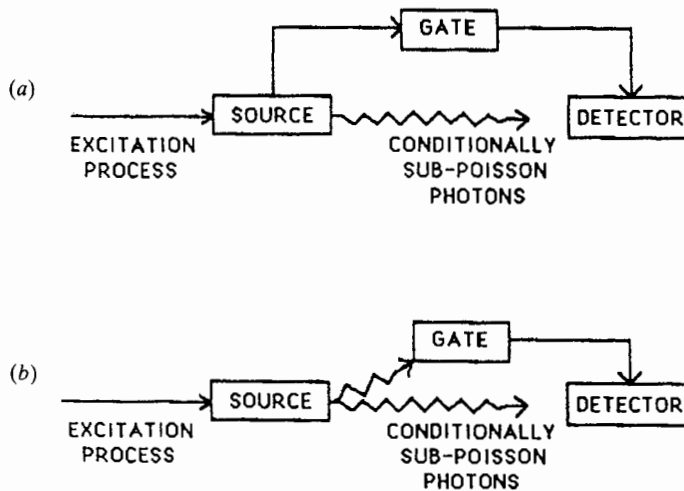


Figure 23. Schematic diagram illustrating the generation of conditionally photon-number-squeezed light. (a) Configuration for atomic resonance fluorescence where the entry of a single atom into the field of view of the apparatus gates the detector open for a brief time. (b) Configuration for correlated photon pairs (e.g. spontaneous parametric downconversion or ^{40}Ca correlated photon emissions), where one partner of a photon pair gates the detector open for a brief time (from [15], reprinted with permission from North Holland publishing).

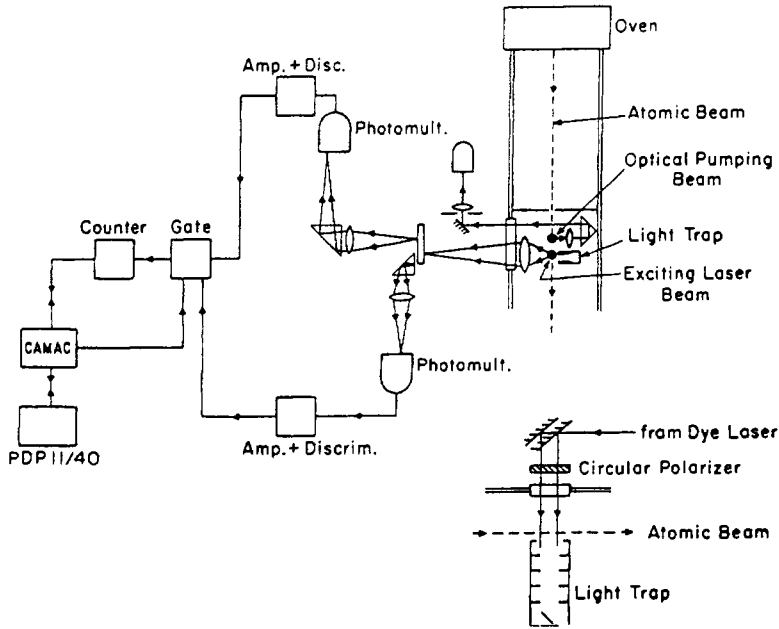


Figure 24. Experimental apparatus for the generation of conditionally photon-number-squeezed resonance fluorescence photon clusters from isolated Na atoms (from [28], reprinted with permission from Plenum publishing).

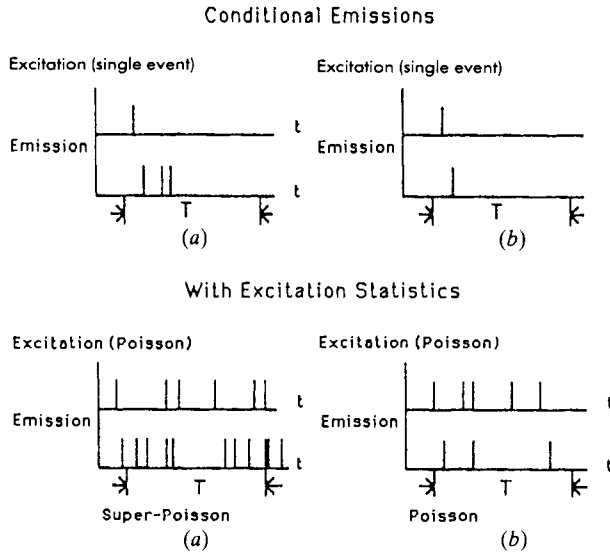


Figure 25. Conditional photon-number squeezing is destroyed by the excitation statistics. Top (a): Sample function for a conditionally photon-number-squeezed resonance-fluorescence photon cluster. Bottom (a): Poisson entries of atoms into the apparatus and unsynchronised gating result in unconditionally super-Poisson resonance-fluorescence radiation. Top (b): Sample function for a conditionally photon-number-squeezed ^{40}Ca violet photon emission. Bottom (b): Poisson entries of ^{40}Ca atoms into the apparatus and unsynchronised gating lead to unconditionally Poisson green and violet photons (from [15], reprinted with permission from North-Holland publishing).

prespecified time window to ensure that it is responsive only during the time period when an anticorrelated number of photons is expected to arrive. This requires knowledge of when this will happen. Nonlinear optics mechanisms (atomic resonance fluorescence [11, 28] and parametric downconversion) can generate small clusters of such photons, e.g. two or three photons for resonance fluorescence from an isolated atom in a typical experiment (figure 24) or a single photon for parametric downconversion. Unfortunately, conditional photon-number squeezing is destroyed by the random excitation statistics when the detector gating is eliminated, as illustrated in figure 25.

Unconditionally photon-number-squeezed light can be generated by the use of either photon feedback or excitation feedback to introduce anticorrelations into the photon occurrence times. The detector is not gated. The former method is discussed first. *Photons* generated by a given process are fed back to control it; this may be accomplished by using a variety of nonlinear-optics techniques. Methods using feedback intrinsic to a physical process (figure 26(a)), simply stated, remove selected clusters of photons from the incident pump beam, leaving behind an antibunched residue (as illustrated in figure 22(c)). External feedback can also be used to achieve this (figure 26(b)).

A simple example is a process in which photon pairs are produced, with one member of the pair being used to control its twin (figure 27). Control mechanisms such as decimation, dead-time deletion, and rate compensation, all illustrated in figure 22, can be used to accomplish these ends. Two techniques for achieving this are portrayed in figures 28 and 29. The first (figure 28) is a suggested configuration that makes use of cascaded atomic emissions [30]. A photon from the initial (green) atomic transition is detected in the conventional manner to provide an external feedback

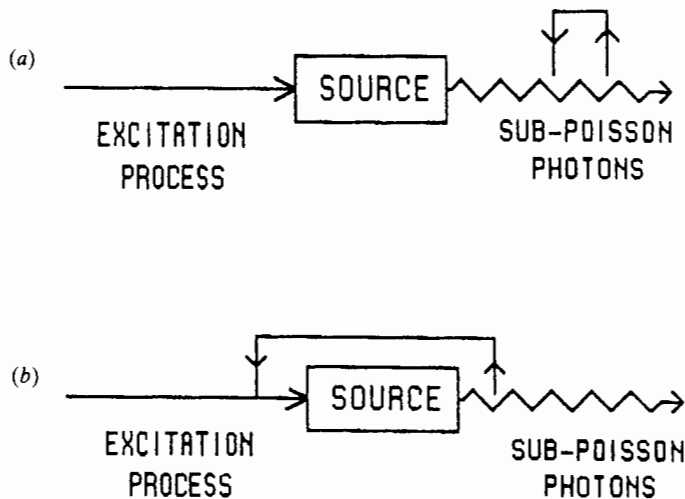


Figure 26. Schematic diagram illustrating the generation of unconditionally photon-number-squeezed light by means of photon feedback. (a) Feedback process intrinsic to a physical light-generation mechanism. (b) Feedback process carried by way of an external path. The feedback may take the form of an electrical signal or an optical signal (from [15], reprinted with permission from North-Holland publishing).

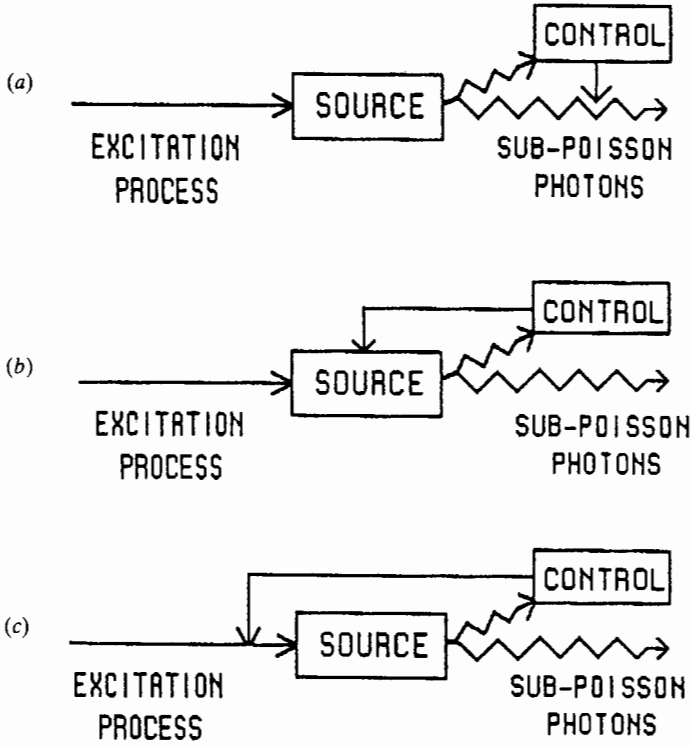


Figure 27. Schematic diagram illustrating the generation of unconditionally photon-number-squeezed light by correlated photon pairs (photon clones) and external feedback. One of the twin photon beams is annihilated to generate the control signal. (a) Optical control of one beam by its twin; (b) photon-source control; (c) excitation control (from [15], reprinted with permission from North-Holland publishing).

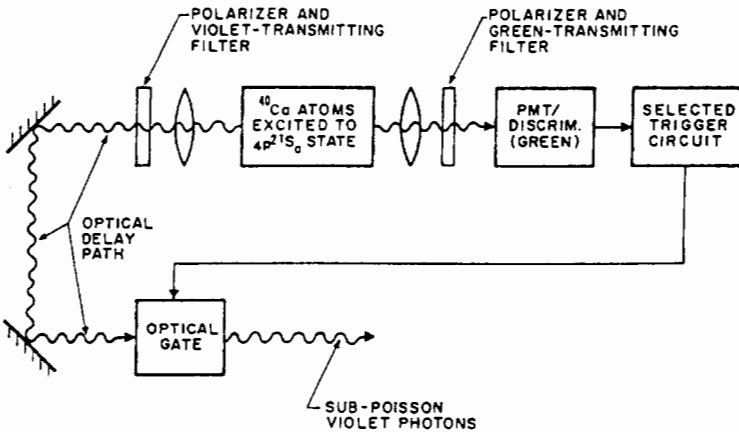


Figure 28. Suggested configuration for the generation of unconditionally photon-number-squeezed light using correlated photon pairs, in this case cascaded photon emissions from ^{40}Ca atoms (from [30], reprinted with permission from North-Holland publishing).

signal. This signal is used selectively to permit certain photons from the second atomic transition (violet) to pass through an optical gate (for example, by means of the decimation process illustrated in figure 22(d)). Since the photons are always emitted in correlated pairs, the selected twins survive and contribute to the light at the output. This experiment is of the type represented in figure 27(a). The second technique, which has been experimentally implemented [31, 32], makes use of parametric down-conversion (figure 29). This effect may be described as the splitting of a single photon into two (correlated) photons of lower frequency. The experiment used an electro-optic modulator to provide analog rate compensation of the pump power (see figure 22(f)) provided by the control beam. Thus, this experiment is of the type represented in figure 27(c). It is worthy of mention that a two-mode optical parametric oscillator operating *above* threshold has been used to generate high-intensity twin beams exhibiting strong quantum correlations [33].

Finally, in the context of photon feedback, we mention a scheme for generating photon-number-squeezed light using a quantum-nondemolition (QND) measurement, by means of which an observable may be measured without perturbing its free motion. It has been proposed by Yamamoto and his co-workers [34] that the results of a QND photon-flux measurement at the output of a semiconductor diode injection laser could be negatively fed back to control the laser excitation rate (figure 30), thereby producing photon-number-squeezed light by rate compensation in the manner shown in figure 22(f). In principle, the feedback signal could be obtained from a probe laser in conjunction with a Kerr nonlinear interferometer, as shown in figure 30. The QND principle has indeed been experimentally verified, but in a different configuration [35].

We now turn to excitation feedback, which provides an alternative technique for generating unconditionally photon-number-squeezed light. In this case, the excitation process itself is rendered sub-Poisson by means of feedback, as illustrated schematically in figure 31 (compare with figure 26 for photon feedback). The feedback

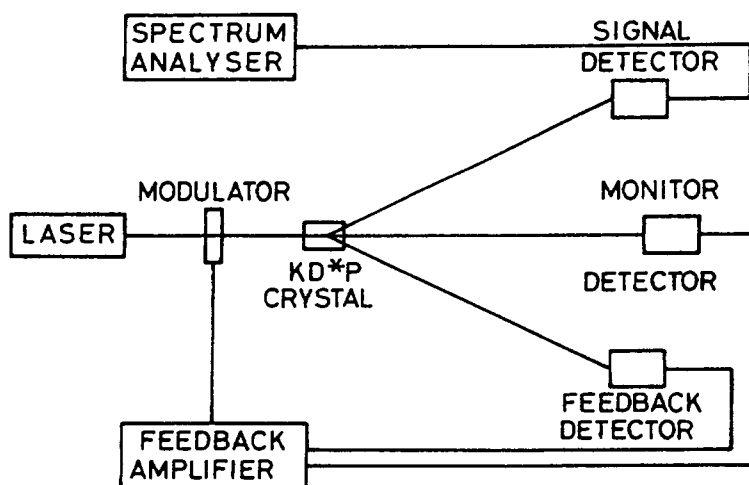


Figure 29. Block diagram for photon-number-squeezed light generation using correlated photon pairs, in this case from parametric downconversion (from [32], reprinted with permission from the American Physical Society).

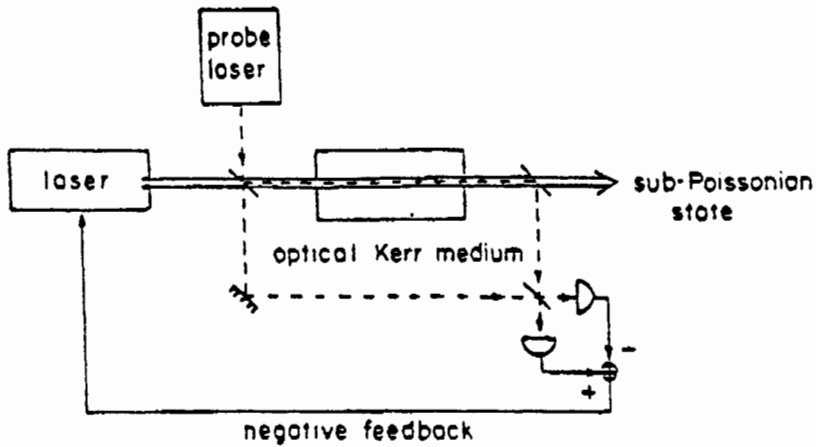


Figure 30. Proposed scheme for generating photon-number-squeezed light using a quantum-nondemolition (QND) measurement of the laser-output photon number to control the laser excitation rate (from [34], reprinted with permission from the American Physical Society).

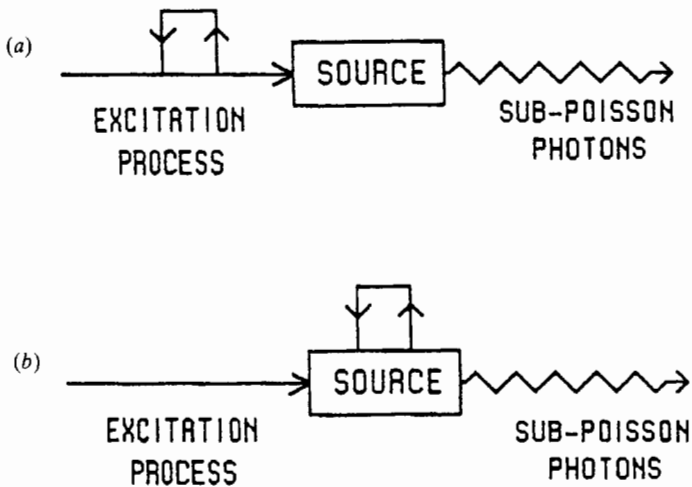


Figure 31. Schematic diagram illustrating the generation of unconditionally photon-number-squeezed light by means of excitation feedback: (a) feedback process intrinsic to a physical excitation mechanism; (b) feedback process intrinsic to the source. Excitation feedback can also be carried externally (from [15], reprinted with permission from North-Holland publishing).

mechanism may be either intrinsic to a physical process or external. Some of the limitations inherent in photon-feedback mechanisms are avoided by the use of excitation feedback [15]. Excitation-feedback methods provide the greatest promise for producing sources with low Fano factor, large photon flux, high overall efficiency, small size, and the capability of being modulated at high speeds. Excitation feedback methods are also referred to as 'direct generation methods'.

Such methods operate by permitting a sub-Poisson number of excitations (e.g. electrons) to generate a sub-Poisson number of photons; the photons may be viewed as representing a nondestructive measurement of the electron number. This is to be distinguished from the QND configurations mentioned earlier in which a sub-Poisson number of photons causes an electrical current to be generated as a result of a phase measurement, which in turn signals the photon number (without destroying the photons). It is far easier to achieve a measurement of the electron number than the photon number because of the robustness of the electrons. Unlike photons, they are not destroyed by optical measurement techniques.

Several excitation-feedback methods have made use of the inherent sub-Poisson nature of an electron current. Coulomb repulsion, which is the underlying physical feedback process in space-charge-limited current flow, is ubiquitous when excitations are achieved by means of electrons. Single-photon emissions (ideally, one per electron) may be obtained in any number of ways. One example is spontaneous fluorescence emission, as shown in figure 32 for Hg vapour. The first source of unconditionally photon-number-squeezed light was produced in a space-charge-limited Franck-Hertz experiment [14], as illustrated in this figure. A block diagram of the experimental apparatus is presented in figure 33.

Unfortunately the loss of photons, as a result of imperfect photon generation, collection, and detection, randomises the statistical properties of anticorrelated excitations, as shown in figure 34. If the losses are sufficiently severe, random (Poisson) photons will be generated. Effects such as attenuation, scattering and the presence of background photons reduce the degree of photon-number (and quadrature) squeezing, and must therefore be assiduously avoided.

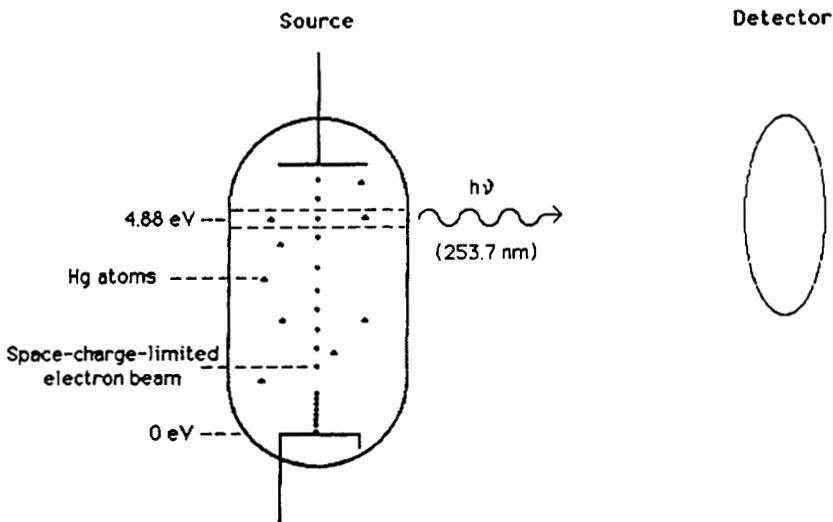


Figure 32. Schematic representation of the generation of unconditionally photon-number-squeezed light using the space-charge-limited Franck-Hertz effect in Hg vapour (from [13], reprinted with permission from the Optical Society of America).

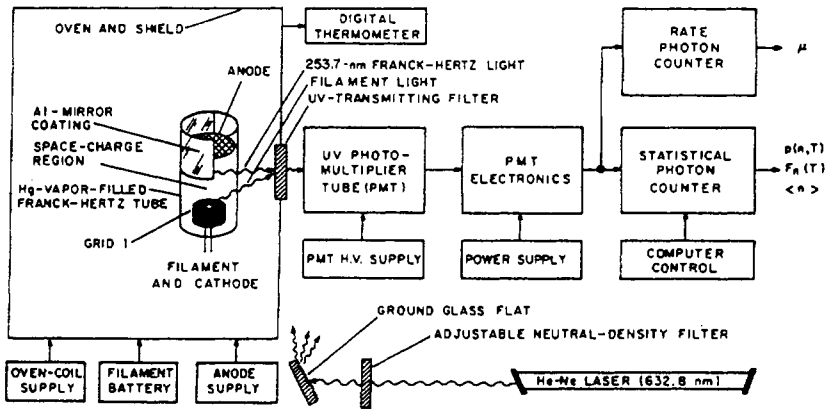


Figure 33. Block diagram of the space-charge-limited Franck-Hertz experimental apparatus that produced the first source of unconditionally photon-number-squeezed light. The wavelength of the light was 253.7 nm in the ultraviolet (from [14], reprinted with permission from the Optical Society of America).

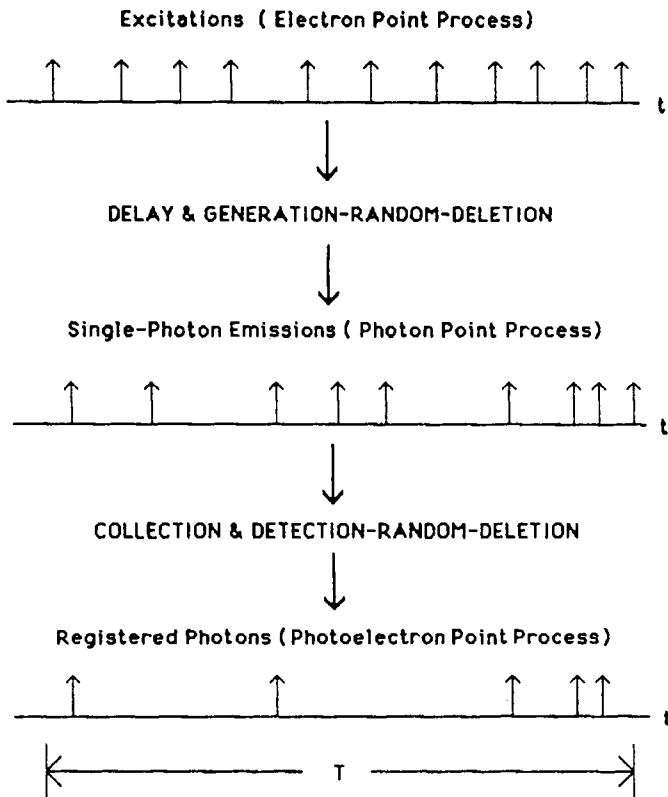


Figure 34. Schematic illustration of photon-number-squeezed light generation using excitation feedback. Photon loss has a deleterious effect on the degree of photon-number- and quadrature-squeezing.

Because of this, several high-collection-efficiency, solid-state, excitation-feedback configurations were developed. Current supplied from a DC source, such as a battery for example, is naturally sub-Poisson as a result of the intrinsic Coulomb repulsion of the electrons (the principal source of noise is Johnson noise). In such cases it suffices to drive a light emitter that operates by means of single photon transitions with such a current. Thus, a simple light-emitting diode (LED), driven by a constant current source, should emit photon-number-squeezed light. Tapster, Rarity, and Satchell [36] have shown that this is indeed the case. Their experiment, which is shown in figure 35, is a solid-state analogue of the space-charge-limited Franck–Hertz experiment. The series resistor serves to ensure that a constant-current source drives the LED. Similarly, a constant-current-driven semiconductor injection laser (figure 36), which is analogous to a stimulated-emission version of the space-charge-limited Franck–Hertz experiment [37], also behaves in this manner [38].

Fast response (small electron anticorrelation time τ_e) is one of the desirable characteristics for photon-number squeezing. The characteristic anticorrelation time τ_f in external feedback circuits may be larger than that for space-charge-limited electron excitations (τ_e). The observation (counting) time T , and area A , must be sufficiently large in comparison with the appropriate characteristic times and spatial extent, respectively, and the generation efficiency η as close to unity as possible, to achieve optimal squeezing.

These considerations have led us to propose a semiconductor device structure in which sub-Poisson electron excitations are attained through space-charge-limited current flow, and single-photon emissions are achieved by means of recombination radiation [39]. A device of this nature would emit unconditionally photon-number-squeezed recombination radiation. One possible energy-band diagram for such a space-charge-limited light-emitting device (SCL-LED) is illustrated in figure 37. Sub-Poisson electrons are directly converted into sub-Poisson photons, as in the space-charge-limited Franck–Hertz experiment, but these are now recombination photons

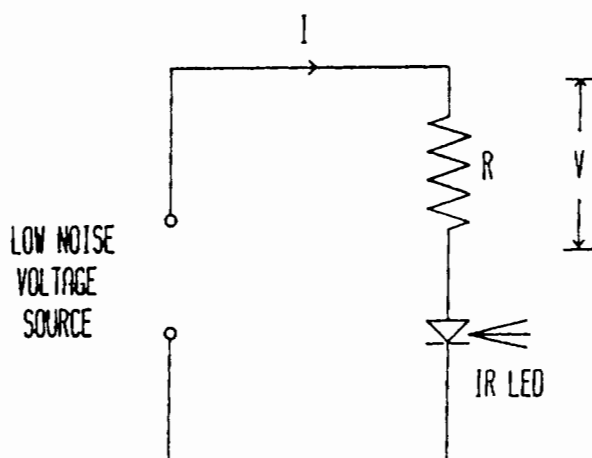


Figure 35. Block diagram of the constant-current-driven light-emitting diode (LED) used to generate unconditionally photon-number-squeezed light (from [36], reprinted with permission from the European Physical Society).

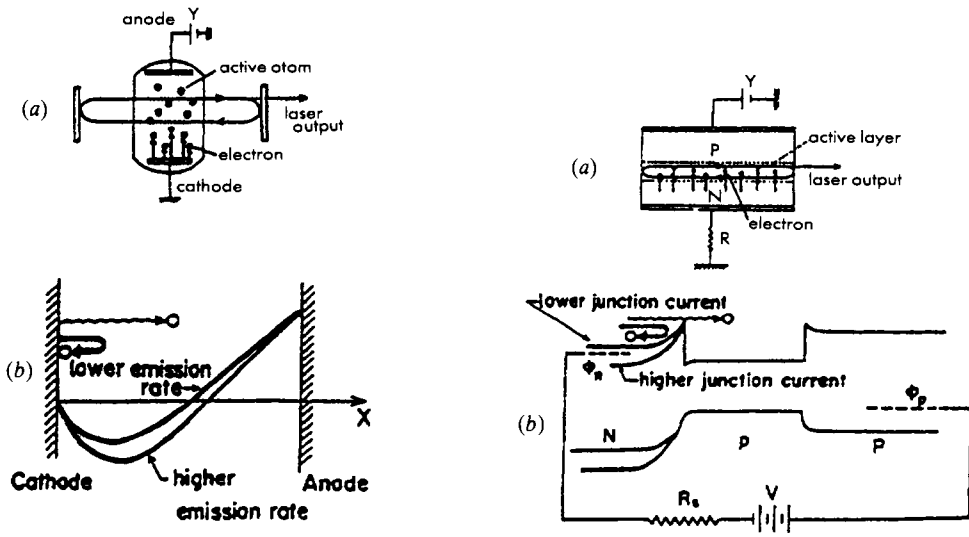


Figure 36. Conceptual suppression of the fluctuations of active atoms in a space-charge-limited Franck-Hertz laser (left). Photon-number-squeezed light generation by suppression of electron pump fluctuations in a constant-current-driven semiconductor injection laser (right) (from [37], reprinted with permission from the American Physical Society).

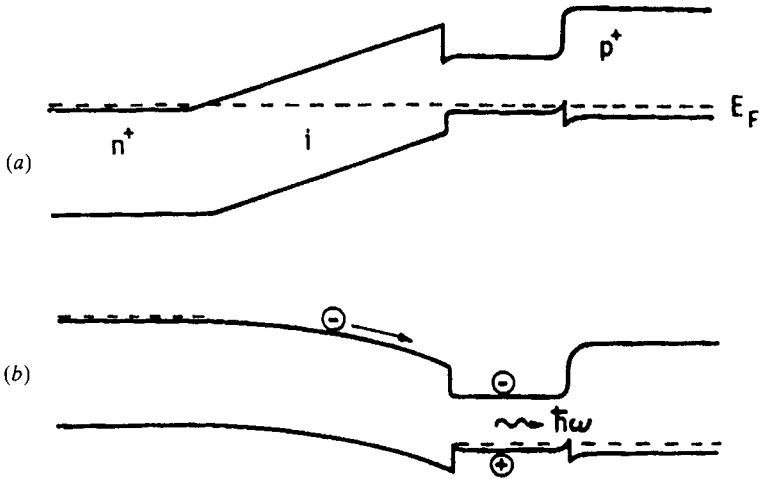


Figure 37. Possible energy-band diagram of a solid-state space-charge-limited light-emitting device (LED or laser) under (a) equilibrium conditions and (b) strong forward-bias conditions. The curvature of the intrinsic region under forward-bias conditions indicates the space-charge potential (from [39], reprinted with permission from the Optical Society of America).

in a semiconductor. The properties of the light generated by the SCL-LED can be enhanced by permitting stimulated emissions to occur. Advantages would include improved beam directionality, switching speed, spectral properties and coupling efficiency to an optical fibre.

10. Early nonclassical light experiments

A list of early experiments in which nonclassical light was generated is provided in table 1. The experimental activity was initiated in 1977 by the observation of photon antibunching in a single-atom resonance fluorescence [29]. Conditional photon-number squeezing was observed in 1983, also from single-atom resonance fluorescence [11]. The first source of unconditional photon-number-squeezed light was generated

Table 1. Early nonclassical light experiments.

YEAR	EFFECT	EXPERIMENT	SOURCE
1977	Photon antibunching	Single-atom resonance fluorescence	Kimble, Dagenais & Mandel <i>Phys. Rev. Lett.</i> 39 691 (1977)
1983	Conditional photon-number squeezing	Single-atom resonance fluorescence	Short & Mandel <i>Phys. Rev. Lett.</i> 51 384 (1983)
1985	Photon-number squeezing	Space-charge-limited Franck-Hertz effect	Teich & Saleh <i>J. Opt. Soc. Am. B</i> 2 275 (1985)
1985	Quadrature squeezing of the vacuum	Nondegenerate four-wave mixing in Na atoms	Slusher, Hollberg, Yurke, Mertz & Valley <i>Phys. Rev. Lett.</i> 55 2409 (1985)
1986	Quadrature squeezing of the vacuum	Nondegenerate four-wave mixing in an optical fibre	Shelby, Levenson, Perlmutter, Devoe & Walls <i>Phys. Rev. Lett.</i> 57 691 (1986)
1986	Quadrature squeezing of the vacuum	Parametric downconversion in MgO:LiNbO ₃	Wu, Kimble, Hall & Wu <i>Phys. Rev. Lett.</i> 57 2520 (1986)
1987	Quadrature squeezing of the vacuum	Nearly degenerate four-wave mixing in Na vapour	Maeda, Kumar & Shapiro <i>Opt. Lett.</i> 12 161 (1987)
1987	Quadrature squeezing of the vacuum	Coupling-induced mode splitting in Na atoms	Raizen, Orozco, Xiao, Boyd & Kimble <i>Phys. Rev. Lett.</i> 59 198 (1987)
1987	Photon-number squeezing	Constant-current-driven semiconductor laser	Machida, Yamamoto & Itaya <i>Phys. Rev. Lett.</i> 58 1000 (1987)
1987	Photon-number squeezing	Parametric downconversion in KD*P	Rarity, Tapster & Jakeman <i>Opt. Commun.</i> 62 201 (1987)
1987	Photon-number squeezing	Constant-current-driven light-emitting-diode	Tapster, Rarity & Satchell <i>Europhys. Lett.</i> 4 293 (1987)

in 1985 using the space-charge-limited Franck-Hertz experiment [14]. Quadrature squeezing of the vacuum, via both four-wave and three-wave mixing, was achieved shortly thereafter [21–25]. In 1987, unconditionally photon-number-squeezed light was produced by a specially fabricated constant-current-drive semiconductor injection laser [38], by a parametric downconversion device [31] and by a constant-current-driven light-emitting diode [36].

11. Applications of squeezed light

Aside from its intrinsic usefulness in carrying out fundamental experiments in optical physics, there are a number of general areas in which the use of quadrature- and/or photon-number-squeezed light may be advantageous. These include spectroscopy [40], interferometry [41], precision measurement [17, 42], light-wave communications [15, 43, 44] and visual science [45]. Quantum fluctuations can limit the sensitivity of certain experiments in all of these areas. We briefly discuss three examples where the use of photon-number-squeezed light might prove beneficial, in the areas of light-wave communications and visual science.

An idealised direct-detection light-wave communication system is illustrated in figure 38. Errors (misses and false alarms) can be caused by noise from many sources, including photon noise intrinsic to the light source. The use of photon-number-squeezed light in place of coherent light can bring about a reduction in this noise, and

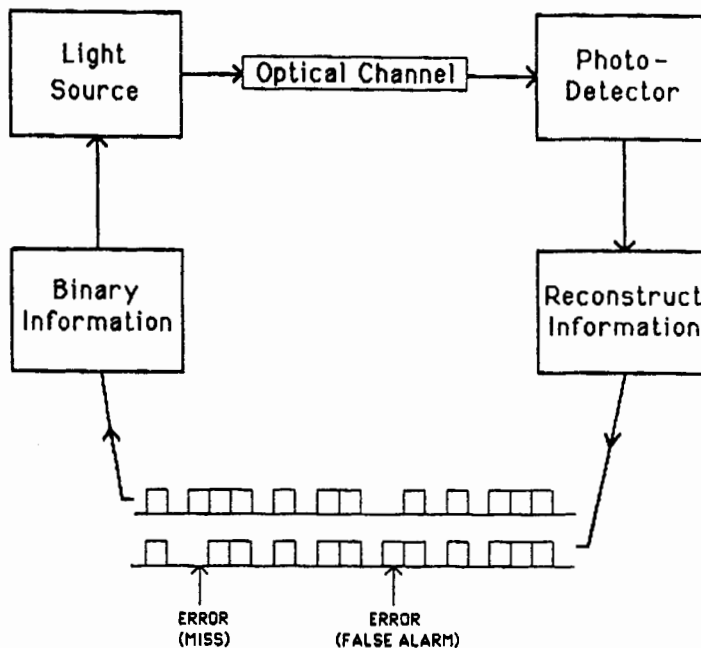


Figure 38. Idealised direct-detection binary ON–OFF keying light-wave communication system. Potential sources of noise include: photon noise, background light, cosmic-ray-induced Čerenkov light, coupling partition noise, photodetector dark noise, photodetector avalanche (multiplication) noise and electronic (Johnson) noise.

thereby the probability of error, as shown schematically in figure 39. For a coherent source, each pulse of light contains a Poisson number of photons so that the photon-number standard deviation $\sigma_n = \langle n \rangle^{1/2}$. For photon-number-squeezed light, each pulse contains a sub-Poisson number of photons so that $\sigma_n < \langle n \rangle^{1/2}$. This noise reduction results in a decrease in the error probability. The mean number of photons per bit $\langle n' \rangle$ required to achieve an error probability of 10^{-9} , in a simple binary ON-OFF keying system whose only source of noise is binomial photon counts (with Fano factor F_n), is shown in figure 40. As the Fano factor decreases below unity, $\langle n' \rangle$ decreases below its coherent-light ($F_n = 1$) 'quantum limit' of 10 photons/bit.

Photon-number-squeezed light may also prove to be a useful tool in visual science. The use of such light could, for example, help to clarify the functioning of the mammalian retinal ganglion cell (figure 41). This cell sends signals to higher visual centres in the brain via the optic nerve. In response to light, the ganglion cell generates a neural discharge that consists of nearly identical electrical events occurring along the time axis (the ganglion-cell discharge point process). The statistical

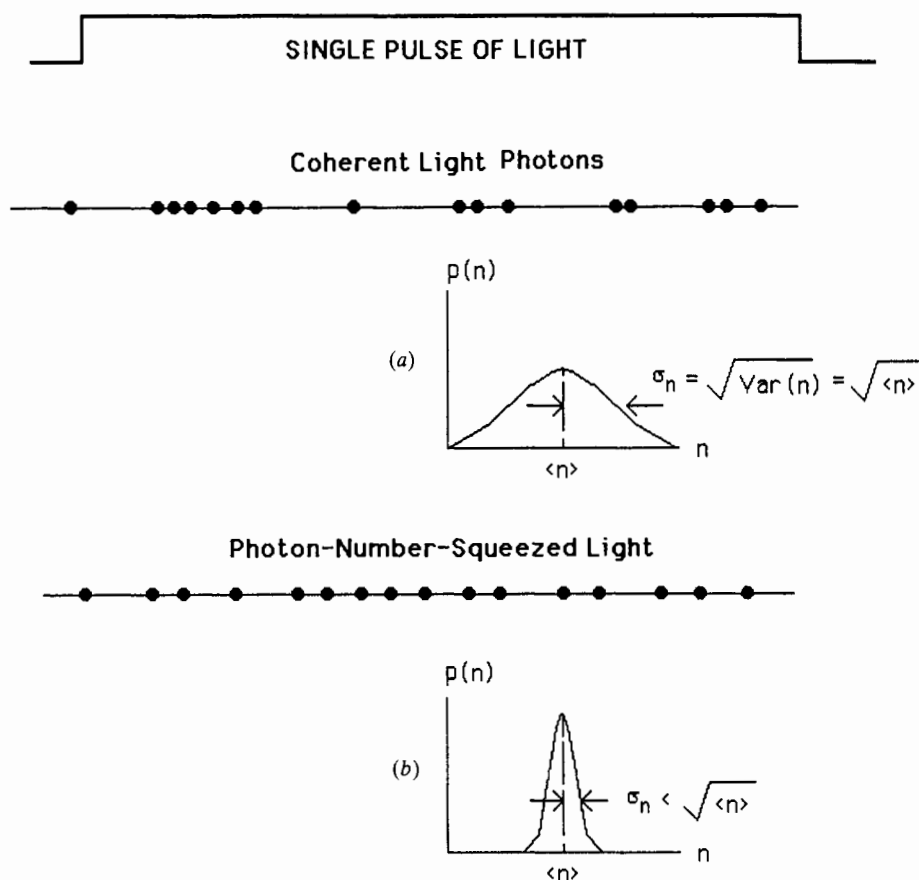


Figure 39. Direct-detection light-wave communications using (a) coherent, and (b) photon-number-squeezed light. The photon occurrences in a single pulse of light are shown schematically.

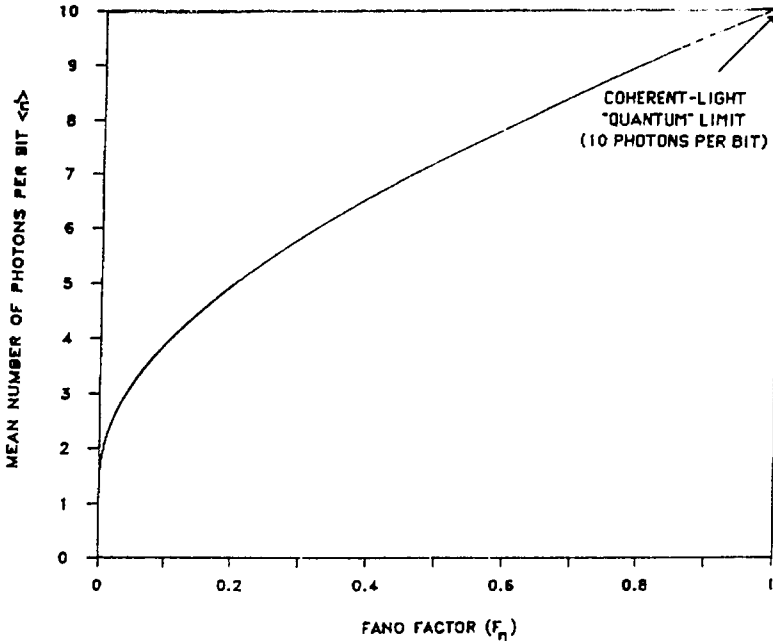


Figure 40. Direct-detection binary on-off keying (OOK) photon-counting system sensitivity using photon-number-squeezed light. It is assumed that the photon-number distribution is binomial, that there are no sources of noise other than photon noise, and that the bit error probability is 10^{-9} (from [15], reprinted with permission from North-Holland publishing).

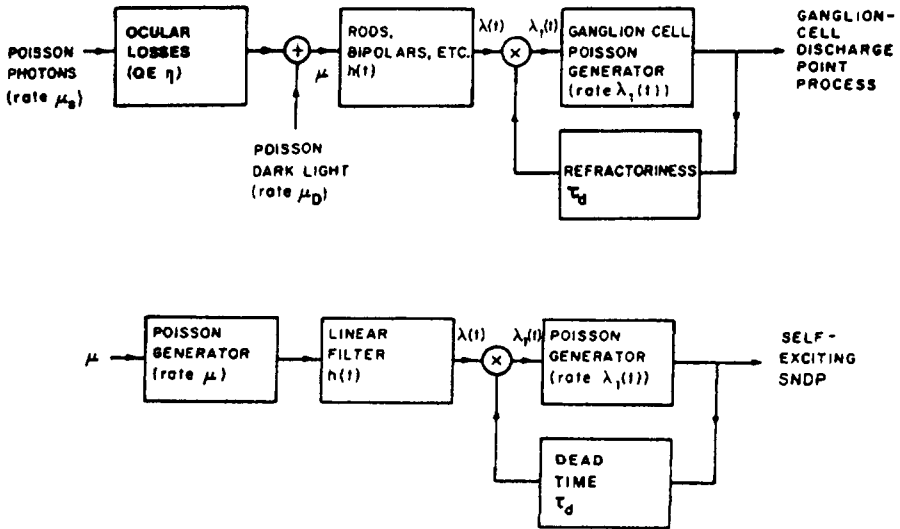


Figure 41. Potential use of photon-number-squeezed light in studying the behaviour of the mammalian retinal ganglion cell (from [46], reprinted with permission from Springer-Verlag).

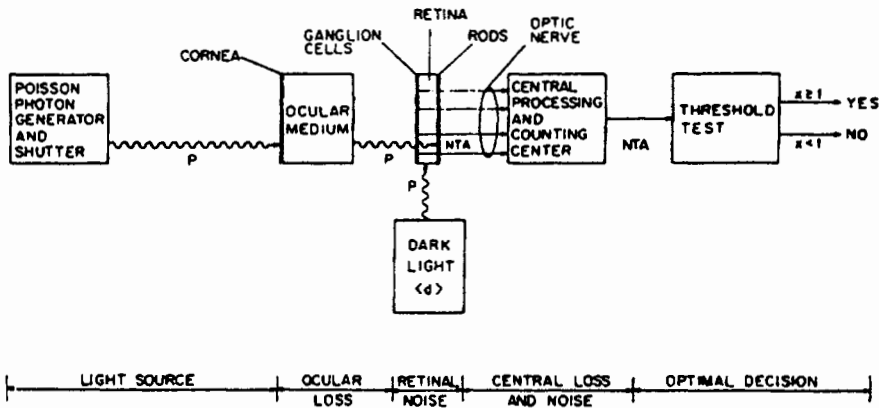


Figure 42. Potential use of photon-number-squeezed light in determining the relative rôles of photon noise, retinal noise and neural noise in the visual response at threshold (from [45], reprinted with permission from Springer-Verlag).

nature of this discharge is assumed to be governed by two elements of stochasticity: the incident photons (which are Poisson distributed in all experiments to date) and a randomness intrinsic to the cell itself (which is sometimes taken to be dead-time-modified Poisson) [46]. If the statistical fluctuations of the photons could be controlled by exciting the retina with photon-number-squeezed light, the essential nature of the randomness intrinsic to the cell could be unambiguously determined.

The outcome of an experiment in visual psychophysics is the (verbal) response of the entire organism rather than the electrical response of a single cell. It is widely assumed that Poisson photon fluctuations govern the uncertainties inherent in the human visual response near the threshold of seeing [47] but substantial retinal and central neural noise is also present (figure 42) [45]. The use of photon-number-squeezed light as a stimulus could clarify the roles played by these distinct sources of noise.

12. Available general literature

A list of general literature in the area of squeezed states of light is given at the end of the list of references. Two recent special journal issues were devoted exclusively to the topic. A number of review articles is also available. The first six listed are devoted to quadrature-squeezed light; the last reviews recent progress in photon-number-squeezed light.

Acknowledgements

This work was supported by the Joint Services Electronics Program through the Columbia Radiation Laboratory and by the National Science Foundation. The article is adapted from a tutorial presented at the 1987 Annual Meeting of the Optical Society of America (Rochester, New York, USA) and at the 1988 Topical Meeting on Photon Correlation Techniques and Applications (Washington, DC, USA).

References

- [1] Glauber R J 1963 *Phys. Rev.* **130** 2529; 1963 *Phys. Rev.* **131** 2766
- [2] Takahasi H 1965 *Advances in Communications Systems: Theory and Applications* vol. 1 ed. A V Balakrishnan (New York: Academic); Robinson D R 1965 *Commun. Math. Phys.* **1** 159; Stoler D 1970 *Phys. Rev.* **D1** 3217; Stoler D 1971 *Phys. Rev.* **D4** 1925; Lu E Y-C 1971 *Lett. Nuovo Cimento* **2** 1241; Lu E Y-C 1972 *Lett. Nuovo Cimento* **3** 585; Yuen H P 1975 *Phys. Lett.* **51A** 1; Yuen H P 1976 *Phys. Rev. A* **13** 2226; Hollenhorst J N 1979 *Phys. Rev. D* **19** 1669
- [3] Walls D F 1983 *Nature* **306** 141
- [4] Shapiro J H 1985 *IEEE J. Quant. Electron.* **QE-21** 237
- [5] Caves C M 1986 'Amplitude and phase in quantum optics' in *Coherence, Cooperation, and Fluctuations* ed. F. Haake, L M Narducci and F Walls (Cambridge: Cambridge University Press)
- [6] Loudon R and Knight P L 1987 *J. Mod. Opt.* **34** 709
- [7] 1987 Special issue of *J. Mod. Opt.* **34**
- [8] 1987 Special issue of *J. Opt. Soc. Am. B* **4**
- [9] Slusher R E and Yurke B 1988 *Sci. Am.* **258** (No. 5) 50
- [10] Henry R W and Glotzer S C 1988 *Am. J. Phys.* **56** 318
- [11] Short R and Mandel L 1983 *Phys. Rev. Lett.* **51** 384
- [12] Teich M C, Saleh B E A and Stoler D 1983 *Opt. Commun.* **46** 244
- [13] Teich M C, Saleh B E A and Peřina J 1984 *J. Opt. Soc. Am. B* **1** 366
- [14] Teich M C and Saleh B E A 1985 *J. Opt. Soc. Am. B* **2** 275
- [15] Teich M C and Saleh B E A 1988 'Photon bunching and antibunching,' in *Progress in Optics* vol. 26, ed. E. Wolf E (Amsterdam: North-Holland)
- [16] Yamamoto Y, Machida S, Imoto N, Kitagawa M and Björk G 1987 *J. Opt. Soc. Am. B* **4** 1645
- [17] Caves C M 1981 *Phys. Rev. D* **23** 1693
- [18] Yuen H P and Chan V W S 1983 *Opt. Lett.* **8** 177; *ibid.* **8** 345
- [19] van de Stadt H 1974 *Astron. Astrophys.* **36** 341
- [20] Yuen H P and Shapiro J H 1979 *Opt. Lett.* **4** 334
- [21] Slusher R E, Hollberg L W, Yurke B, Mertz J C and Valley J F 1985 *Phys. Rev. Lett.* **55** 2409
- [22] Shelby R M, Levenson M D, Perlmutter S H, DeVoe R G and Walls D F 1986 *Phys. Rev. Lett.* **57** 691
- [23] Wu L-A, Kimble H J, Hall J L and Wu H 1986 *Phys. Rev. Lett.* **57** 2520
- [24] Maeda M W, Kumar P and Shapiro J H 1987 *Opt. Lett.* **12** 161
- [25] Raizen M G, Orozco L A, Xiao M, Boyd T L and Kimble H J 1987 *Phys. Rev. Lett.* **59** 198
- [26] Wu L-A, Xiao M and Kimble H J 1987 *J. Opt. Soc. Am. B* **4** 1465
- [27] Peřina J 1985 *Coherence of Light*, 2nd edn (Dordrecht: Reidel); 1984 *Quantum Statistics of Linear and Nonlinear Optical Phenomena* (Dordrecht: Reidel)
- [28] Short R and Mandel L 1984 'Sub-Poissonian photon statistics in resonance fluorescence' in *Coherence and Quantum Optics V*, ed. L Mandel and E Wolf (New York: Plenum) p. 671
- [29] Kimble H J, Dagenais M and Mandel L 1977 *Phys. Rev. Lett.* **39** 691
- [30] Saleh B E A and Teich M C 1985 *Opt. Commun.* **52** 429
- [31] Rarity J G, Tapster P R and Jakeman E 1987 *Opt. Commun.* **62** 201
- [32] Tapster P R, Rarity J G and Satchell J S 1988 *Phys. Rev. A* **37** 2963
- [33] Heidmann A, Horowicz R J, Reynaud S, Giacobino E and Fabre C 1987 *Phys. Rev. Lett.* **59** 2555
- [34] Yamamoto Y, Imoto N and Machida S 1986 *Phys. Rev. A* **33** 3243
- [35] Levenson M D, Shelby R M, Reid M and Walls D F 1986 *Phys. Rev. Lett.* **57** 2473
- [36] Tapster P R, Rarity J G and Satchell J S 1987 *Europhys. Lett.* **4** 293
- [37] Yamamoto Y, Machida S and Nilsson O 1986 *Phys. Rev. A* **34** 4025
- [38] Machida S, Yamamoto Y and Itaya Y 1987 *Phys. Rev. Lett.* **58** 1000; Machida S and Yamamoto Y 1988 *Phys. Rev. Lett.* **60** 792
- [39] Teich M C, Capasso F and Saleh B E A 1987 *J. Opt. Soc. Am. B* **4** 1663
- [40] Yurke B and Whittaker E A 1987 *Opt. Lett.* **12** 236; Carmichael H J, Lane A S and Walls D F 1987 *Phys. Rev. Lett.* **58** 2539
- [41] Xiao M, Wu L-A and Kimble H J 1987 *Phys. Rev. Lett.* **59** 278; Grangier P, Slusher R E, Yurke B and LaPorta A 1987 *Phys. Rev. Lett.* **59** 2153
- [42] Gea-Banacloche J and Leuchs G 1987 *J. Mod. Opt.* **34** 793
- [43] Yuen H P and Shapiro J H 1978 *IEEE Trans. Inf. Theory* **IT-24** 657; Shapiro J H, Yuen H P and Machado Mata J A 1979 *IEEE Trans. Inf. Theory* **IT-25** 179; Yuen H P and Shapiro J H 1980 *IEEE Trans. Inf. Theory* **IT-26** 78

- [44] Saleh B E A and Teich M C 1987 *Phys. Rev. Lett.* **58** 1656; Yamazaki K, Hirota O and Nakagawa M 1988 *Trans. IEICE (Japan)* **71** 775
- [45] Teich M C, Prucnal P R, Vannucci G, Breton M E and McGill W J 1982 *Biol. Cybern.* **44** 157
- [46] Saleh B E A and Teich M C 1985 *Biol. Cybern.* **52** 101
- [47] Hecht S, Shlaer S and Pirenne M H 1942 *J. Gen. Physiol.* **25** 819

General literature on squeezed states of light

Special journal issues devoted to squeezed states

Journal of Modern Optics **34** (June/July 1987)

Journal of the Optical Society of America B **4** (October 1987)

Review articles

Walls D F 1983 *Nature* **306** 141

Shapiro J H 1985 *IEEE J. Quant. Electron.* **QE-21** 237

Caves C M 1986 in *Coherence, Cooperation, and Fluctuations* (a symposium in honour of Roy J. Glauber, Harvard University, 1985) ed. F. Haake, L M Narducci and D F Walls (Cambridge: Cambridge University Press)

Loudon R and Knight P L 1987 *J. Mod. Opt.* **34** 709

Slusher R E and Yurke B 1988 *Sci. Am.* **258** (No. 5) 50

Henry R W and Glotzer S C 1988 *Am. J. Phys.* **56** 318

Teich M C and Saleh B E A 1988 in *Progress in Optics* **26** 1 ed. E Wolf (Amsterdam: North-Holland)